This paper has been published under the following reference: Ahmadi, E., Caprani, C., Živanović, S. and Heidarpour, A. (2018) Vertical ground reaction forces on rigid and vibrating surfaces for vibration serviceability assessment of structures. *Engineering Structures*, Vol. 172, pp. 723-738. (https://doi.org/10.1016/j.engstruct.2018.06.059)

Vertical ground reaction forces on rigid and vibrating surfaces for vibration serviceability assessment of structures

Ehsan Ahmadi[a], Colin Caprani[a*], Stana Živanović[b], and Amin Heidarpour[a]

[a] Dept. of Civil Engineering, Monash University, Australia

[b] School of Engineering, University of Warwick, UK

*Corresponding author: colin.caprani@monash.edu

Abstract

Lightweight structures are sensitive to dynamic force generated by human walking and consequently can exhibit excessive vibration responses. The imparted forces, known as ground reaction forces (GRFs), are a key input in the vibration serviceability assessment of footbridges. Most GRF measurements have been conducted on rigid surfaces such as instrumented treadmills and force plates mounted on strong floors. However, it is thought that the vibrating surface of a footbridge might affect the imparted human force. This paper introduces a unique laboratory experimental setup to investigate vertical GRFs on both rigid surface (strong floor) and a higher frequency flexible surface (footbridge). 810 walking trials were performed by 18 test subjects walking at different pacing frequencies. For each trial, test subjects travelled a circuit of a vibrating footbridge surface followed by a rigid surface. A novel data collection setup was adopted to record the vertical component of GRFs, and the footbridge vibration response during each trial. Frequency-domain analysis of both single-step and continuous GRFs was then performed. The results show that the footbridge vibration affects GRFs, and changes GRF magnitudes for harmonics in resonance with the footbridge vibration (up to around 30% reduction in the dynamic load factor of the third harmonic). This finding, and the measured GRFs, can be used for more accurate vibration serviceability assessments of existing and new footbridges.

Keywords: Footbridges; Vibration; Human; GFRP; Ground reaction forces; Dynamic load factors.

1. Introduction

1.1. Background

Due to their increasingly slender nature, many modern structures are prone to excitation from human activity. Human activities such as walking, running, jumping, and bouncing, can cause uncomfortable vibrations, potentially leading to reduced usage of the facility. Among these activities, walking is a key consideration for footbridge vibration. For low-frequency structures having one or more natural frequencies within range of first harmonic of walking force (1.6–2.4 Hz), walking at a pacing frequency close to the natural frequency of the structure might cause a vibration response that is considered uncomfortable by bridge users. The vibration response of a footbridge is generally largest if the resonance is excited by the first harmonic of walking force. For structures with natural frequencies within range of higher harmonics of walking force (larger than about 3.2 Hz – "higher-frequency"), the resonance by the second or third forcing harmonic might also be significant, even though the force amplitudes are smaller. To investigate higher-frequency vibration effects, extensive walking experiments were conducted on a higher-frequency footbridge for which the first frequency is in resonance with the third harmonic of walking force.

This paper has been published under the following reference: Ahmadi, E., Caprani, C., Živanović, S. and Heidarpour, A. (2018) Vertical ground reaction forces on rigid and vibrating surfaces for vibration serviceability assessment of structures. *Engineering Structures*, Vol. 172, pp. 723-738. (https://doi.org/10.1016/j.engstruct.2018.06.059)

1.2. Ground reaction forces

To have a good prediction of footbridge vibration response, accurate estimation of the input walking force and reliable modelling of the structure are required. The former is the focus of this study. Humans apply an approximately periodic time-dependent force with vertical, lateral, and longitudinal components, referred to as ground reaction force (GRF) [1–3]. The vertical GRF has two distinctive peaks at heelstrike and toe-off phases, and a trough at mid-stance phase for one step during walking, as shown in Fig. 1. The vertical GRF has received much attention by previous researchers [4–19].

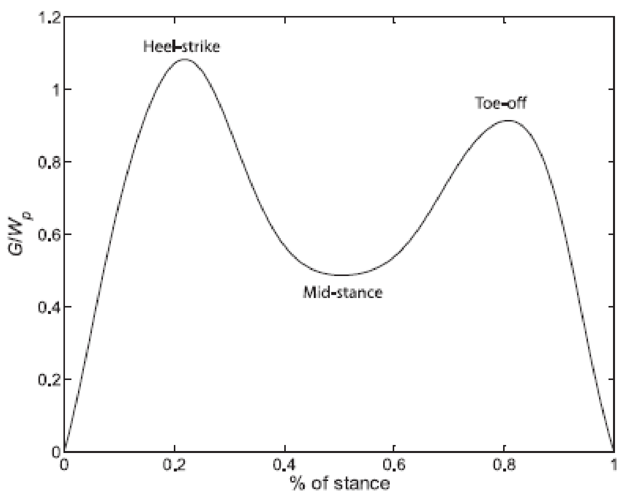

Figure 1: Typical shape of a vertical GRF for a single step in walking.

In the time domain, continuous walking GRFs are commonly described using a Fourier series [20–23]:

$$G_c(t) = W_p \sum_{k=0}^{r} DLF_k \cos(2\pi k f_p t + \varphi_k) \qquad (1)$$

where $W_p=m_p g$ and m_p is the pedestrian mass, g is the acceleration due to gravity; f_p is the walking pacing frequency; and DLF_k is the dynamic load factor (DLF) for the kth harmonic. The phase angle of the kth harmonic is denoted by φ_k, and r represents total number of harmonics considered. In this representation, the harmonic k=0 corresponds to the static pedestrian weight, and so φ_0=0 and DLF_0=1.

This paper has been published under the following reference: Ahmadi, E., Caprani, C., Živanović, S. and Heidarpour, A. (2018) Vertical ground reaction forces on rigid and vibrating surfaces for vibration serviceability assessment of structures. *Engineering Structures*, Vol. 172, pp. 723-738. (https://doi.org/10.1016/j.engstruct.2018.06.059)

All GRF studies explained so far originate from GRF measurements on rigid surface. These GRFs were measured by force plates and instrumented treadmills placed on rigid floors. This leaves the possibility that the reported vertical GRFs could be different to those that actually occur on lively footbridges, i.e. they could be affected by the vertical movement of the walking surface. Only a few works in the past have considered this. Ohlsson [24] reported that the spectrum of the walking force showed a drop around the natural frequency of the structure where the response was significant. Baumann and Bachmann [25] similarly reported DLFs of walking force, which were around 10% lower on the vibrating surface. However, they measured only single footsteps by a force plate mounted on a 19m prestressed beam of frequency 2.3 Hz ("low-frequency bridge"). Pimentel [26] also suggested 10% and 40% reductions respectively in the first and second DLFs of the walking force by matching measured vibration responses with those calculated from an updated finite element (FE) model using a moving force model for two test subjects; but DLF models based on rigid surface measurements were used, and no GRFs were measured on the vibrating footbridge. In a unique study, Dang and Živanović [27] studied the influence of vertical vibration on vertical GRFs using an instrumented treadmill on a low-frequency laboratory footbridge. The results show that the footbridge vibration reduces vertical GRFs at the first harmonic of resonant walking. However, only a limited number of test subjects walked on-the-spot for this study, and it is limited to a footbridge with frequency at the first harmonic of the walking force ("low-frequency bridge"). To conclude, the literature lacks measurements of GRFs due to walking on vibrating bridge surfaces, particularly for higher-frequency footbridges for a large range of test subjects. The aim of the paper is to address this gap using a novel experimental set-up.

1.3. Lightweight high-frequency footbridges

Glass fibre reinforced polymer (GFRP) material is increasingly applied in the construction industry for its desirable properties such as high strength-to-weight ratio and good durability in extreme environments. These properties make GFRP well suited to modular structural forms such as floors and footbridges. However, GFRP structures are lighter than equivalent conventional structures, rendering them potentially more susceptible to human-induced vibration due to a higher accelerance amplitude (acceleration response per unit harmonic force) [28]. Therefore, a GFRP footbridge was designed and built to establish the performance of such structures, and the influence of structural vibration on GRFs.

The vibration design rules for FRP footbridges have evolved from experience with steel and concrete structural forms [29,30]. The AASHTO Design Guideline for FRP Footbridges [29] states that bridges with a first natural frequency greater than 5 Hz are deemed acceptable for vibration serviceability. However, this seems to neglect the altered mass-stiffness relationship of FRP when compared with traditional steel and concrete structures. The altered relationship affects the magnitude of the accelerance function. Živanović et al. [31] compared accelerance functions of several FRP footbridges against comparable steel/concrete footbridges. The accelerance functions of Monash University laboratory GFRP footbridge—uncovered and covered (to be described later)—have been added to those presented by Živanović et al. [31], and they are shown in Fig. 2. In addition, the frequency ranges for first three walking harmonics are shown shaded, along with the 5 Hz limit [29]—shown as red dashed line in the same figure.

Fig. 2 shows that the GFRP footbridges (AB, EB, MBu, MBc) exhibit higher accelerance compared to other footbridges. Given that vibration response increases when the natural frequencies lie in the harmonic ranges excitable by human normal walking, these footbridges

This paper has been published under the following reference: Ahmadi, E., Caprani, C., Živanović, S. and Heidarpour, A. (2018) Vertical ground reaction forces on rigid and vibrating surfaces for vibration serviceability assessment of structures. *Engineering Structures*, Vol. 172, pp. 723-738. (https://doi.org/10.1016/j.engstruct.2018.06.059)

could have vibration serviceability design problems. Interestingly, the 5 Hz frequency limit, developed many decades ago from experience with steel and concrete structures has been adopted in AASHTO [29]. As seen in Fig. 2, the purpose-built Monash Bridge (MB) was designed to meet the 5 Hz limit. The resulting bridge has a natural frequency within the range excitable by the third harmonic of walking force and creates opportunity to critically evaluate the suitability of the 5 Hz limit for lightweight structures.

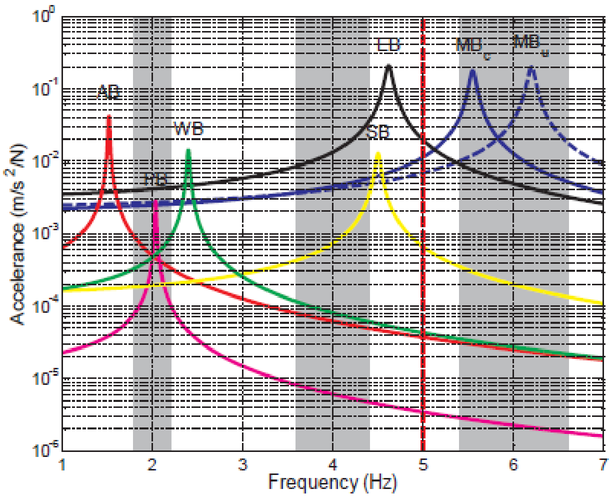

Figure 2: First mode accelerance frequency response functions (FRFs) of different footbridges, walking harmonics (Shaded grey), and the 5 Hz limit. AB – Aberfeldy Footbridge (GFRP), PB – Podgoricia Bridge (Steel), WB – Warwick Bridge (Steel-Concrete Composite), SB – Sheffield Bridge (Prestressed Concrete), EB – EMPA Bridge (GFRP deck), MBu – Monash Bridge, uncovered (GFRP), and MBc – Monash Bridge, covered (some data from [31]).

1.4. Contribution

Although most GRF models are based on data collected on rigid surfaces, it is the GRFs imparted on the actual bridge surfaces, which are typically flexible, that are of most interest for predicting the vibration response of lively structures reliably. Further, higher-frequency lightweight footbridges ought to be studied, as resonance with higher harmonics of the walking force might result in a large vibration response despite the bridge satisfying the 5 Hz limit. To address these two goals, reliable measurement of vertical GRFs on both rigid and a higher- frequency vibrating bridge surface is conducted. A higher-frequency lightweight

This paper has been published under the following reference: Ahmadi, E., Caprani, C., Živanović, S. and Heidarpour, A. (2018) Vertical ground reaction forces on rigid and vibrating surfaces for vibration serviceability assessment of structures. *Engineering Structures*, Vol. 172, pp. 723-738. (https://doi.org/10.1016/j.engstruct.2018.06.059)

laboratory footbridge—the Monash University GFRP footbridge – is instrumented with three devices to simultaneously record vertical GRFs and vibration responses. A novel instrumentation set-up is used to measure full time history GRFs and single footstep GRFs on both the footbridge and rigid surfaces. Finally, frequency-domain analysis of single-step GRFs and continuous walking GRFs (dynamic load factors) are carried out for both surfaces to infer potential effects of vibration on the harmonics of vertical walking force. The ultimate goal is that these effects can then be incorporated into future vibration severability checks which will not be addressed in this study.

2. Experimental setup

2.1. Description of Monash GFRP footbridge

The deck of the Monash University GFRP footbridge is a sandwich panel made from pultruded GFRP box sections placed between two GFRP flat sheets as shown in Fig. 3a. The 1.5m wide orthotropic deck sits on two pultruded FRP I-beam girders, spanning 8.7m between supports. All components of the footbridge are joined using epoxy bonding to ensure full composite action. No bolted connections or steel components were used. Bidirectional fibre orientations for flat sheets, box sections, and I-beam girders were adopted to maximize strength and stiffness in both transverse and longitudinal directions as shown in Fig. 3b. The Monash University GFRP footbridge has a mass of 92.5 kg/m (61.6 kg/m2). This makes it very lightweight compared to more traditional structures, for example, the steel-concrete composite Warwick University laboratory footbridge which has a mass of 829 kg/m [27].

Fig. 4 shows the first three modes of the uncovered footbridge structure, MBu, from an impact hammer test. The first mode is a flexural mode having natural frequency of 6.0 Hz and damping ratio of 0.6%. The second mode is a torsional mode with frequency of 10.0 Hz

This paper has been published under the following reference: Ahmadi, E., Caprani, C., Živanović, S. and Heidarpour, A. (2018) Vertical ground reaction forces on rigid and vibrating surfaces for vibration serviceability assessment of structures. *Engineering Structures*, Vol. 172, pp. 723-738. (https://doi.org/10.1016/j.engstruct.2018.06.059)

and damping ratio of 1.0%. The third mode is the second bending mode with frequency of 18.1 Hz and 0.6% damping ratio.

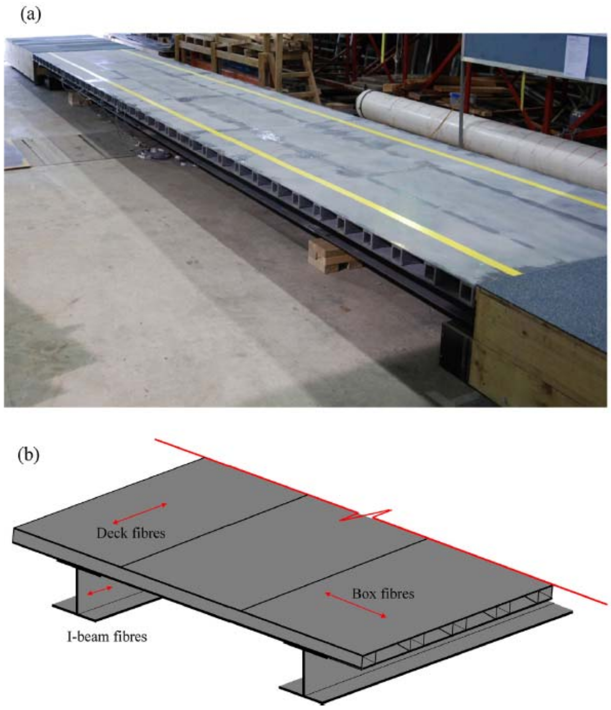

Figure 3: Monash GFRP footbridge: (a) footbridge structure with end walkways, and (b) fibre direction of different components.

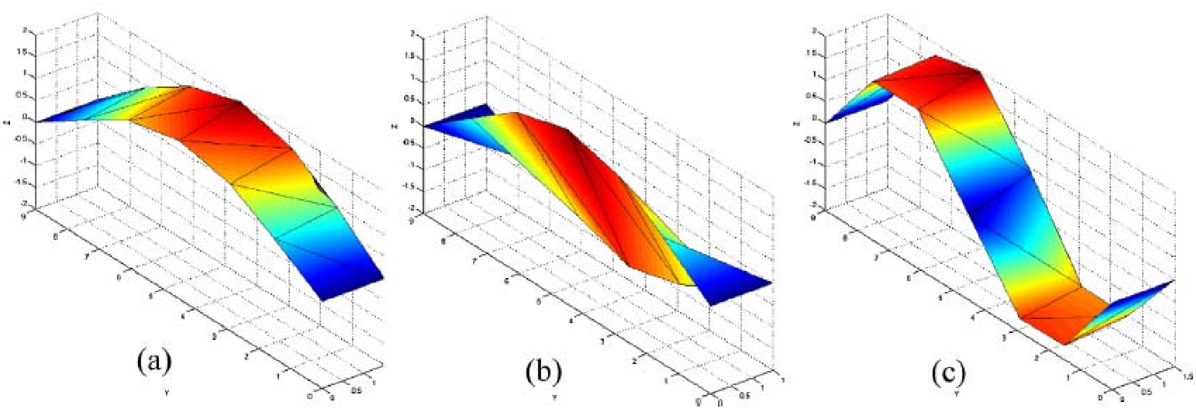

Figure 4: Experimental modal analysis of the footbridge: (a) first bending mode, 6.0 Hz and 0.6% damping ratio, and (b) first torsional mode, 10.0 Hz and 1.0% damping ratio; (c) second bending mode, 18.1 Hz and 0.6% damping ratio.

This paper has been published under the following reference: Ahmadi, E., Caprani, C., Živanović, S. and Heidarpour, A. (2018) Vertical ground reaction forces on rigid and vibrating surfaces for vibration serviceability assessment of structures. *Engineering Structures*, Vol. 172, pp. 723-738. (https://doi.org/10.1016/j.engstruct.2018.06.059)

2.2. Experiment setup for the bridge surface

Measurements of GRFs and structural vibration responses are key elements to human-induced vibration studies. A unique experimental setup was designed to measure GRFs and bridge acceleration. The uniqueness of the study is in measuring GRFs using three independent measurement approaches: a force plate, load cells at the supports, and a state-of-the-art in-shoe plantar pressure recording system (see Fig. 5).

A 400 wide×600 long×75mm high BERTEC FP4060-07 force plate, was placed on the footbridge surface at the mid-span, 200mm off the bridge centreline, towards the left edge, where the force plate is highly likely hit by test subjects' foot. Such force plates are commonly used for gait analysis. They consist of force transducers that measure six force components: three orthogonal forces and the moments about the three axes [32]. The force plate mass, natural frequency, maximum vertical load capacity, and resolution are 38 kg, 340 Hz, 5 kN, and±0.5 N, respectively [32].

Four C10 HBM load cells were placed in the supports at the four ends of the GFRP I-beams. They are capable of measuring both tensile and compressive forces up to 25 kN with accuracy class of 0.04% (e.g. maximum of load cell deviations specified as percentage) and have a resonant frequency higher than 5.8 kHz [33]. In the bridge walking experiments, the measured reactions in the supports are used to determine the total vertical force and its instantaneous location on the footbridge.

A state-of-the-art in-shoe pressure measurement system, the Tekscan F-scan, was used to measure GRFs on both bridge and rigid surfaces [34]. These sensors consist of a grid of capacitors, and each sensor measures the plantar pressure on an area of about 15mm2 [34]. Tekscan pressure sensors are used across multiple industries such as medicine, dentistry, and biomechanical research [34–37], for the measurement of contact forces, pressure distribution, and centre of pressure. For walking, the plantar pressure force gives a reliable measurement of the vertical walking force [38,39]. Their accuracy depends on factors such as the calibration method, contact area and contact time with the sensors [40,41].

To measure the vibration response of the footbridge, two DYTRAN 3191A1 accelerometers of nominal sensitivity of 10 V/g were placed at the mid-span on each sides of the bridge deck (A1 and A2 in Fig. 5). They have capability to measure vibration in the frequency range of 0.08–1000Hz, with maximum acceleration of 0.5*g*, and have a resonant frequency above 8kHz.

Due to the additional 75mm height of the force plate on top of the structure deck, the GFRP footbridge structure was covered with additional materials to provide a flush walking surface—the covered footbridge, MBc, of Fig. 2. These materials were carefully selected to provide a stiff walking surface while having little effect on the structure dynamic properties. Consequently, 600 wide×750 long×75mm high Styroboard XPS 250 extruded polystyrene sheets (a stiff foam-like material) were used (Fig. 5). These blocks have nominal density of 35 kg/m^3 and breaking compressive strength of 375 kPa, light and stiff enough for walking purposes. The blocks are not adhered to each other or the bridge, ensuring minimal influence on the structure behaviour. Finally, 3mm medium-density fibreboard (MDFs) was used to finish the walking surface, providing test subjects with a homogenous walking surface across both the footbridge and approach lengths (see Fig. 5). The MDF was placed in 1×1.5m sheets and not adhered to each other or the XPS, so as not to contribute to the longitudinal bending stiffness of the footbridge. It should be noted that this covering eliminates the potential for targeting of the force plate by the test subjects, since they do not know here it is located beneath the MDF. The additional materials and force plate add 106 kg to the uncovered

This paper has been published under the following reference: Ahmadi, E., Caprani, C., Živanović, S. and Heidarpour, A. (2018) Vertical ground reaction forces on rigid and vibrating surfaces for vibration serviceability assessment of structures. *Engineering Structures*, Vol. 172, pp. 723-738. (https://doi.org/10.1016/j.engstruct.2018.06.059)

footbridge to give a total mass of 939 kg for the covered footbridge, MBc, hereafter referred to as the footbridge.

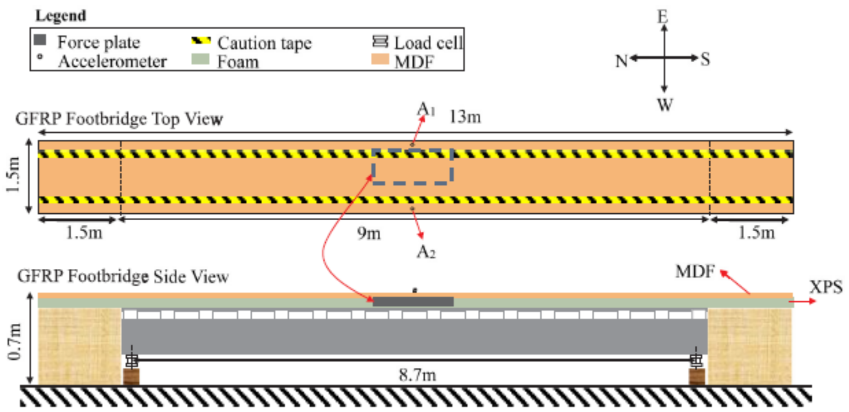

Figure 5: Experiment setup for the bridge walk (A1 and A2 are accelerometers).

2.3. Walking trials procedure

Each trial consists of a bridge surface (BS) walk and a rigid surface (RS) walk, as shown in Fig. 6. Test subjects travel a complete loop to perform one trial. After being given an audio signal, each test subject starts walking from station S1 while looking straight ahead at a target sign in front, traverses the footbridge (near its middle line), and stops at station S2 (bridge surface walk). Afterwards, the test subjects are guided (down the steps) to station S3, from where they perform nominally the same test but this time over the rigid surface, and stop at station S4 (rigid surface walk). A metronome was used to provide an aural cue to assist test subjects maintain the intended pacing frequency.

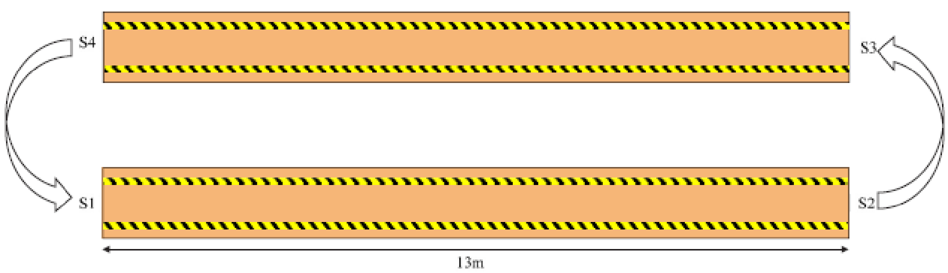

Figure 6: Walking path during each walking trial.

This paper has been published under the following reference: Ahmadi, E., Caprani, C., Živanović, S. and Heidarpour, A. (2018) Vertical ground reaction forces on rigid and vibrating surfaces for vibration serviceability assessment of structures. *Engineering Structures*, Vol. 172, pp. 723-738. (https://doi.org/10.1016/j.engstruct.2018.06.059)

A wide range of 18 test subjects, 9 males and 9 females, participated in the walking trials. Their physical data are listed in Table 1. The weight of test subjects ranges from 444 N to 1489 N and the height ranges from 154 cm to 190 cm. All test subjects were adults in the 20–40 years age range with no reports or indications of medical walking-related problems.

Table 1: Test subjects participated in this study (M and F stand for male and female respectively).

Test subject no.	Height (cm)	Weight (N)	Gender
1	174	865	M
2	172	718	M
3	166	654	M
4	154	444	F
5	181	678	M
6	186	862	M
7	179	717	M
8	175	970	M
9	166	522	F
10	182	1063	M
11	171	647	F
12	173	773	F
13	161	495	F
14	165	609	F
15	164	509	F
16	168	683	F
17	182	1489	F
18	190	1112	M
–	173 ± 9	767 ± 262	–

Before each experiment, all XPS and MDF pieces for the bridge and rigid surfaces were well packed. The mid-span accelerometers were taped to the footbridge MDF surface using double sided tape, and their cables were taped to the sides of the footbridge with sufficient slack. Load cells and force plate readings were zeroed. Before the walking trials for each test subject, an APS 113 ELECTRO series electrodynamic shaker and free decay vibration tests were performed to determine the actual dynamic characteristics of the covered footbridge. This was done since different environmental temperatures and other factors could affect the dynamic properties of the footbridge.

This paper has been published under the following reference: Ahmadi, E., Caprani, C., Živanović, S. and Heidarpour, A. (2018) Vertical ground reaction forces on rigid and vibrating surfaces for vibration serviceability assessment of structures. *Engineering Structures*, Vol. 172, pp. 723-738. (https://doi.org/10.1016/j.engstruct.2018.06.059)

A generic flat-soled canvass shoe was used by all test subjects to eliminate the influence of footwear from the experiment. The trials for each test subject took around 3 h to complete. Fig. 7 shows a test subject instrumented with the Tekscan equipment, consisting of Tekscan sensors, ankle cuffs, data recorder, and cables. A significant effort was made to ensure that the test subject felt comfortable while walking. In particular, the ankle cuffs should not be too tight and the cables from the cuffs to the recorder should be loose enough to allow uninhibited walking. The in-shoe sensors must be flat without any folds or creases. Calibration and zeroing of sensors (explained later in more detail) were performed after each set of 5 consecutive trials to eliminate the potential influence of sensor drift or degradation. The test subjects completed a minimum of 15 trials for each of three pacing frequencies.

Figure 7: Setup of the Tekscan equipment on a test subject.

Before each experiment, comprehensive instructions were given to the test subject and a consent form was signed. To ensure minimal influences of the laboratory environment, the test procedure was followed exactly from a step-by-step workflow, so that all test subjects had a consistent experience. Variations then, are natural of the test subjects, and not of

This paper has been published under the following reference: Ahmadi, E., Caprani, C., Živanović, S. and Heidarpour, A. (2018) Vertical ground reaction forces on rigid and vibrating surfaces for vibration serviceability assessment of structures. *Engineering Structures*, Vol. 172, pp. 723-738. (https://doi.org/10.1016/j.engstruct.2018.06.059)

experimental procedure or environment insofar as is possible. Due to the involvement of human subjects, the experiment was approved by the Monash University Human Research Ethics Committee (Approval no. MUHREC-4455).

2.4. Data collection setup for the bridge surface

Fig. 8 shows the data collection setup for the bridge walk part. A 4-channel DT9838 module was used to record the data from the four load cells [42]. A 16-channel DT9857E module (with high resolution of 24 bits) [42] was used to collect the data from the accelerometers (two channels) and force plate (six channels). Both acquisition modules were directly connected to a computer to store the recorded data. A wireless data-logger unit, worn by the test subjects, was used to record the data from Tekscan F-scan sensors. The data is stored in the data-logger's internal micro-SD memory card for transfer to the computer at a later time (done for each test subject after completing every 5 trials). All of the data was saved in a format suitable for later analysis in MATLAB.

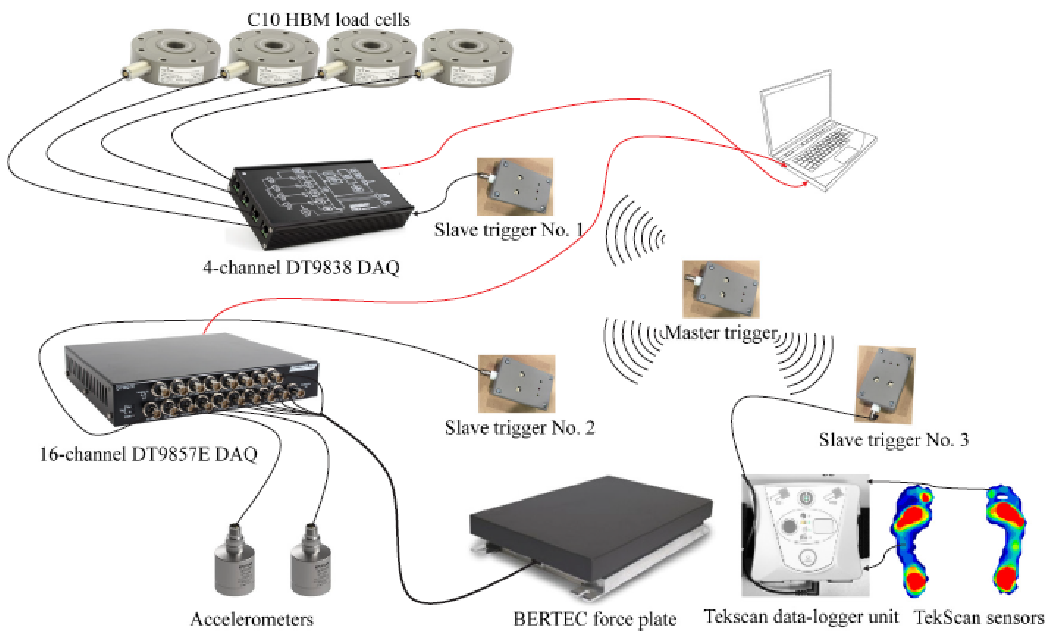

Figure 8: Triggering, instrumentation, and data collection setup for the bridge walk.

This paper has been published under the following reference: Ahmadi, E., Caprani, C., Živanović, S. and Heidarpour, A. (2018) Vertical ground reaction forces on rigid and vibrating surfaces for vibration serviceability assessment of structures. *Engineering Structures*, Vol. 172, pp. 723-738. (https://doi.org/10.1016/j.engstruct.2018.06.059)

QuickDAQ and F-scan software were used to set the acquisition parameters for the DT modules and Tekscan data-logger unit, respectively. Each signal was recorded for 20 s with a sampling frequency of 500 Hz – far above the Nyquist frequency for the vibrations of interest. This measurement period was long enough to capture the crossing event and free decay vibration after the test subjects walked off the footbridge.

A key aspect of the experiment setup is in ensuring time synchronization between the different data acquisition systems by using different triggering methods. To accomplish this, a bespoke set of wireless transceivers were developed, with multiple output signal types, as suited to the input trigger signal for each DAQ. A single master trigger is activated by a button push, which wirelessly triggers each DAQ device simultaneously. When the pre-determined measurement period finishes, the DAQs stop recording automatically. It should be noted that both the DT9838 and DT9857E modules and Tekscan data-logger unit were used to collect the data (Fig. 8) for the walking over the bridge (see Fig. 6). For walking over the rigid surface (see Fig. 6) the Tekscan data-logger unit was used only, but it was still wirelessly triggered for a consistent test subject experience.

3. Preparatory measurements

Preparatory experiments were conducted before the main walking trials for two reasons: (1) to select suitable pacing frequencies for the main trials, and; (2) to ensure accurate measurements for each of the instruments. Specifically, for (2), it was necessary to remove the footbridge vibration effects from the load cells and force plate outputs.

3.1. Pacing frequency selection process

Selection of the pacing frequencies was done empirically by examining the footbridge vibration response under a wide range of pacing frequencies. The resonant pacing frequency, to be targeted in the main experiments, is determined as the pacing frequency that caused the highest possible vibration response. A target non-resonant pacing frequency is also determined; the comparison of resonant and non-resonant responses will give insight in the effects of vibration levels on GRFs. Finally, a normal (uncontrolled) pacing frequency (pacing frequency at which a test subject walks naturally and unprompted by any external stimulus) is used to observe the footbridge liveliness under more natural conditions.

For the selection of pacing frequencies, a test subject carried out five successful walking trials for each pacing frequency between 1.7 Hz and 2.1 Hz with an increment of about 0.017 Hz (1 beat per minute of the metronome setting) around resonance and 0.05 Hz away from resonance. Fig. 9 shows the variation of maximum footbridge response at the mid-span, a_{max}, with test subject pacing frequency, f_p. The vibration of the footbridge is greatest for pacing frequencies between 1.83 Hz and 1.91 Hz. The target pacing frequency (whose third harmonic causes the resonance of the footbridge) is then taken as 1.87 Hz. This is due to two reasons: (1) the first frequency of the covered footbridge, MBc, (5.6 Hz from experimental modal analysis of the covered footbridge) lies in the third harmonic range of the walking force frequency (5.6 Hz/3=1.87 Hz) and (2) during the walking trial experiments, a test subject is likely to walk within a small range of the target pacing frequency, and so 1.87 Hz is selected as it lies within ± 0.04 Hz of the resonant range, shown by red dashed lines in Fig. 9.

A pacing frequency of 1.7 Hz is selected as the target non-resonant pacing frequency as, on average, it gives the lowest response. Therefore, the main trials were conducted for these target resonant, non-resonant, and normal pacing frequencies. For each pacing frequency, 15 acceptable trials were performed to allow for a reliable statistical analysis.

This paper has been published under the following reference: Ahmadi, E., Caprani, C., Živanović, S. and Heidarpour, A. (2018) Vertical ground reaction forces on rigid and vibrating surfaces for vibration serviceability assessment of structures. *Engineering Structures*, Vol. 172, pp. 723-738. (https://doi.org/10.1016/j.engstruct.2018.06.059)

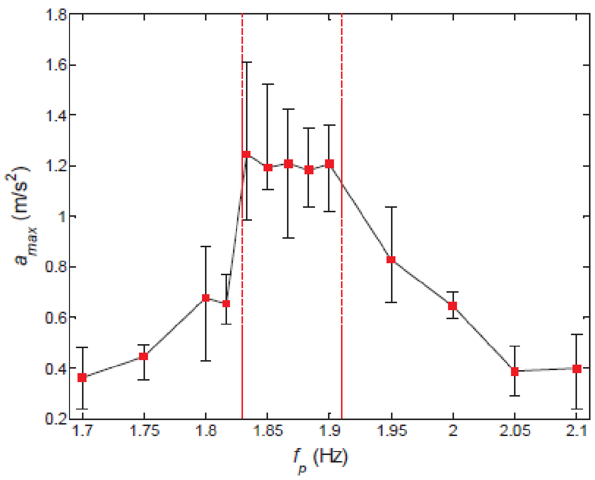

Figure 9: Identification of resonant and non-resonant pacing frequency ranges using vibration responses from 5 trials each at 1.7–2.1 Hz pacing frequencies.

3.2. Effect of footbridge vibration on load cells output

For each trial, the readings of all four load cells are summed to obtain the total force measured by the load cells, *Glc*. Fig. 10a shows a typical G_{lc} signal (back line) for test subject no. 1 (see Table 1) and trial no. 9 at resonance. Note that this specific test subject and trial is used as an example to demonstrate the data analysis procedure and experimental results throughout the paper, and it is referred to hereafter as the "exemplar trial". For the walk over the bridge surface, the total force induced in the load cells consists of the vertical GRFs generated by the walker, GBS, and the inertial force of the footbridge, G_I, due to its vibration (Fig. 10a):

$$G_{lc} = G_I + G_{BS} \tag{2}$$

Using frequency-domain signal processing, say, a notch filter, it is not possible to remove only the bridge inertial force from the load cells' total force measurement because the third harmonic component of walking force would also be filtered out (see acceleration shown in Fig. 10a). Therefore, an alternative approach is developed. Theoretically, considering just the first vertical flexural mode, the total inertial force of the footbridge is:

This paper has been published under the following reference: Ahmadi, E., Caprani, C., Živanović, S. and Heidarpour, A. (2018) Vertical ground reaction forces on rigid and vibrating surfaces for vibration serviceability assessment of structures. *Engineering Structures*, Vol. 172, pp. 723-738. (https://doi.org/10.1016/j.engstruct.2018.06.059)

$$G_I(t) = \int_0^L m(x)\ddot{u}(x)dx = \left[\int_0^L m(x)\phi_1(x)dx\right]\ddot{q}_1(t) = M_I\ddot{q}_1(t) \qquad (3)$$

in which $m(x)$ is the mass distribution of the covered footbridge; $\ddot{u}(x)$ is the acceleration of the footbridge at location x; ϕ_1 (x) is the unit normalized mode shape, and $\ddot{q}_1(t)$ is the modal acceleration. At the midspan ϕ_1 (L/2) = 1 and therefore a measured mid-span acceleration is equal to modal acceleration $\ddot{q}_1(t)$, i.e. $a_b(t) = \ddot{u}(L/2,\, t) = \phi_1(L/2)\ddot{q}_1(t) = \ddot{q}_1(t)$. Thus, Eq. (3) can be rearranged to determine the "inertial mass", M_I , of the footbridge as:

$$M_I = \frac{G_I(t)}{a_b(t)} \qquad (4)$$

Based on this, the inertial mass is calculated using the free decay vibration part of the mid-span acceleration and load cells force signals. During free decay vibration, only the inertial force of the footbridge exists (the test subject has already walked off the footbridge), and thus G_{BS} = 0, which gives Glc = G_I from Eq. (4). Picking peak values of load cell force and acceleration at the mid-span (Fig. 10b) and using Eq. (4), gives a set of inertial mass measurements, shown as black stars in Fig. 10c. As seen in Fig. 10c, these inertial masses are very similar, and the mean inertial mass is found to be M_I = 610 kg.

To determine the third harmonic of the walking force (that has frequency around 5–6 Hz) from load cells, $G_{lc,3h}$, first the measured midspan acceleration of the footbridge, a_b, is filtered by a zero-phase 4th order bandpass Butterworth filter in range of 5–6 Hz to isolate the vibration of the first bending mode of the footbridge. Then, the inertial force of the footbridge during the bridge walk (while the test subject is present on the footbridge) is obtained using Eq. (4) with M_I as determined previously. The load cells force is similarly filtered, $G_{lc,f}$. This force comprises the inertial force of the footbridge, G_I, and the walking force around third harmonic, $G_{lc,3h}$ for the bridge walk part. Thus, the walking force around third harmonic, $G_{lc,3h}$ is obtained from:

This paper has been published under the following reference: Ahmadi, E., Caprani, C., Živanović, S. and Heidarpour, A. (2018) Vertical ground reaction forces on rigid and vibrating surfaces for vibration serviceability assessment of structures. *Engineering Structures*, Vol. 172, pp. 723-738. (https://doi.org/10.1016/j.engstruct.2018.06.059)

$$G_{lc,3h}(t) = G_{lc,f}(t) - G_I(t) \quad (5)$$

An example of the application of these steps is shown in Fig. 11 for the exemplar trial.

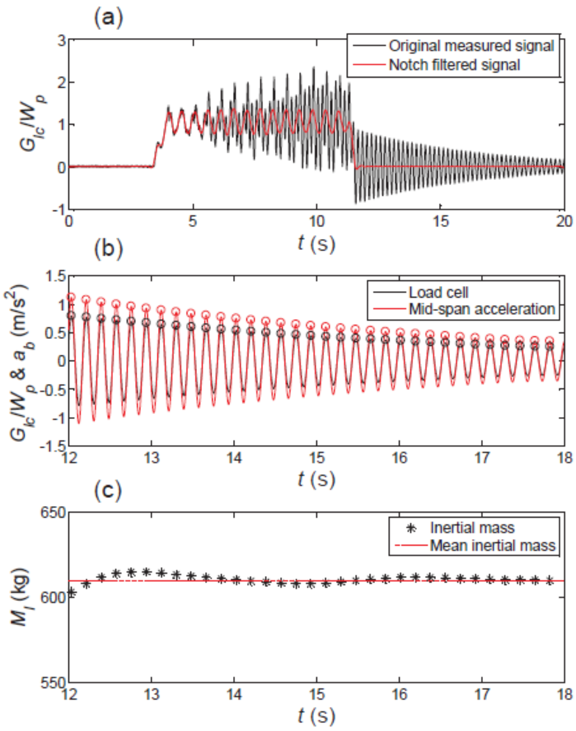

Figure 10: Determination of the inertial mass of the footbridge for the exemplar test subject no 1, trial no 9: (a) original and filtered load cells total force, illustrating that the filtered signal cannot be used, (b) load cells total force and mid-span acceleration for the free decay vibration part, and (c) inertial mass of the footbridge.

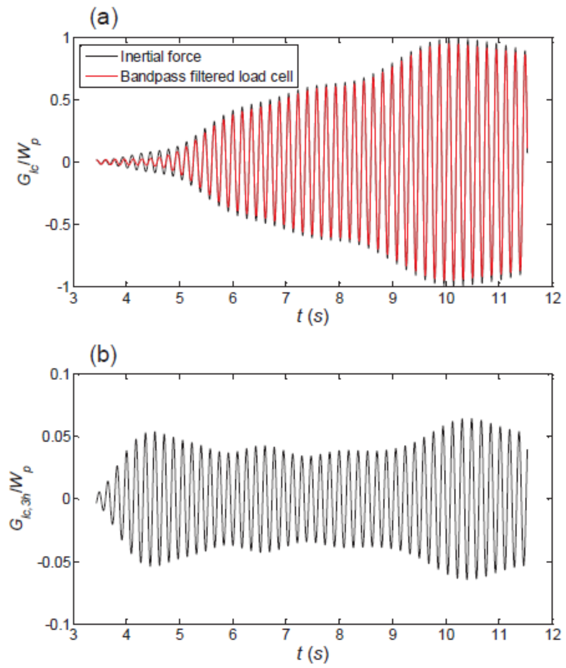

Figure 11: Example extraction of the walking force third harmonic from the load cells: (a) inertial force and filtered load cell, and (b) subtraction of inertial force from filtered load cell.

3.3. Effect of footbridge vibration on force plate output

Fig. 12a shows the force plate reading for the exemplar trial (black line). Some low-amplitude ripples in the original (raw) force plate readings, G_{fp}^{o} , are observed due to the footbridge vibration when the test subject is not on the force plate. Similar to the load cell outputs, using a filter to remove the effect of the footbridge vibration (Fig. 12a, red line) would also remove the third harmonic of the force plate-measured GRFs, which is the quantity of interest.

The inertia force component induced in the force plate due to the footbridge vibration, G_{fp}^{b} , is related to the moving mass of the force plate, M_{fp}, and recorded acceleration, a_{fp}, by:

$$G_{fp}^{b}(t) = M_{fp} a_{fp}(t) \tag{6}$$

To determine this force, both M_{fp} and a_{fp}, must be measured and related to the footbridge mid-span acceleration, a_b. Consequently, two accelerometers were placed, one on the force plate, a_{fp}, and one on the footbridge surface beside the force plate, ab, and the footbridge was excited by the electrodynamic shaker using a swept sine signal with range of frequencies, 1–100 Hz. Fig. 12b shows that the acceleration time histories for both footbridge and force plate are very similar, $a_{fp}=a_b$; this means that there is little relative movement. This can be expected since the force plate natural frequency (340 Hz according to the manufacturer) is far higher than the footbridge natural frequency (5.6 Hz). Therefore, since $a_{fp}=a_b$, the force plate moving mass, M_{fp}, is calculated as 21.3 kg using Eq. (6) (see Fig. 12c).

The identified force-plate moving mass, 21.3 kg, is used to remove the force component induced in the force plate due to the footbridge vibration (Fig. 12c). For each bridge walk, the original force plate reading, G_{fp}^{o} , is used to determine the force plate reading excluding the footbridge vibration effects:

This paper has been published under the following reference: Ahmadi, E., Caprani, C., Živanović, S. and Heidarpour, A. (2018) Vertical ground reaction forces on rigid and vibrating surfaces for vibration serviceability assessment of structures. *Engineering Structures*, Vol. 172, pp. 723-738. (https://doi.org/10.1016/j.engstruct.2018.06.059)

$$G_{fp}(t) = G_{fp}^{0}(t) - M_{fp} a_b(t) \tag{7}$$

where the footbridge acceleration at the mid-span, a_b, is measured for each bridge walk.

The accuracy of the load cells and force plate output was tested using a shaker experiment. The shaker was placed on the force plate and its applied force was compared with the load cells and force plate after removal of vibration effects. The results showed ±3% deviation from the shaker's applied force, which gives confidence in the processing of the force plate and load cells measurements.

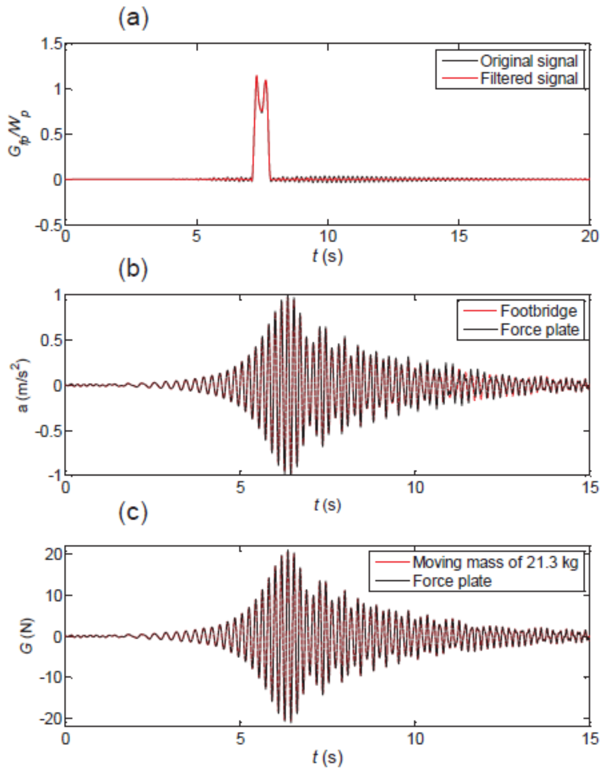

Figure 12: Experiments to remove footbridge vibration effects from force plate: (a) force plate reading during the exemplar trial, (b) force plate and footbridge acceleration in the shaker test, and (c) force plate moving mass calculation.

3.4. Tekscan F-scan force

To measure vertical walking force on both rigid and bridge surfaces during each walking trial experiment, the Tekscan F-scan in-shoe pressure sensors [36,37] were used in this study. In contrast to force plate and instrumented treadmill studies, where test subjects walk on-the-

This paper has been published under the following reference: Ahmadi, E., Caprani, C., Živanović, S. and Heidarpour, A. (2018) Vertical ground reaction forces on rigid and vibrating surfaces for vibration serviceability assessment of structures. *Engineering Structures*, Vol. 172, pp. 723-738. (https://doi.org/10.1016/j.engstruct.2018.06.059)

spot on a rigid (vast majority – see Section 1.2) or bridge surface (e.g. [25,27]), vertical GRFs during each trial on both surfaces were measured. These pressure sensors provide force-time histories for each foot, allowing detailed gait analysis. Tekscan F-scan in-shoe sensors, pressure distribution, and rigid surface force signals for the left and right feet for the exemplar trial are shown in Fig. 13.

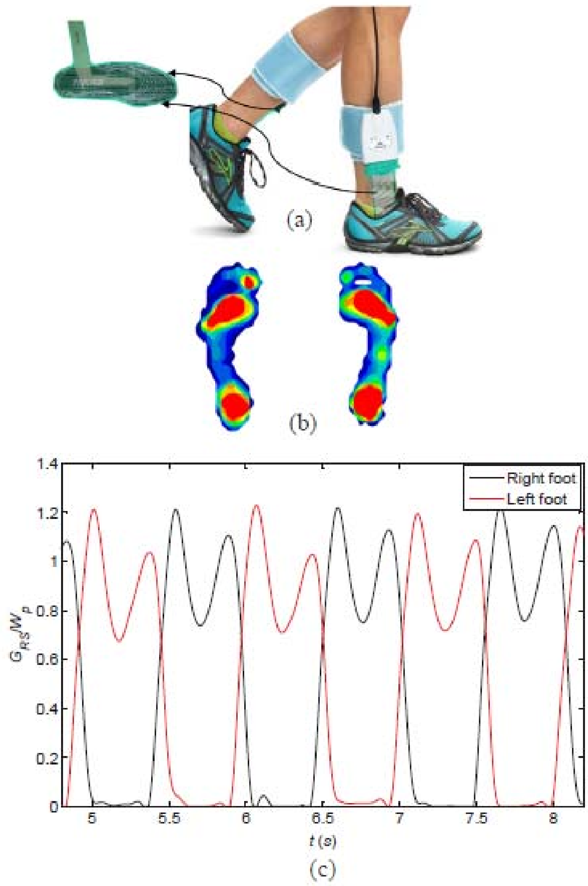

Figure 13: Tekscan F-scan in-shoe sensors: (a) instrument, (b) example output pressure distribution, and (c) calibrated and zeroed integrated force signals of left and right feet for the exemplary test subject on the bridge surface (images (a) and (b) taken from [34]).

The Tekscan in-shoe sensors comprise 960 individual pressure sensing capacitor cells, referred to as sensels. The sensels are arranged in rows and columns on each sensor. The 8-bit output of each sensel is divided into 2^8=256 increments, and displayed as a value, (e.g. Raw Sum) in the range of 0 to 255 by the associated F-scan software. The left and right feet force are shown as raw sum on F-scan software. When all sensors reach a raw count of 255, the corresponding pressure is termed the saturation pressure. The sensor outputs are calibrated to engineering measurement units. Obviously, proper calibration of the sensors is critical to obtaining accurate force readings. It is also necessary to zero the sensor output. Indeed, when one foot is supporting the body weight during walking, the other foot is up in the air and its force reading should be zero. However, because the foot sensors are pre-tensioned to the sole of the foot by shoe-lacing, the output of sensors is not necessarily zero when the foot is not touching the ground. Hence, it is necessary to zero the force output for each trial during a leg swing phase of walking (Fig. 13).

Due to degradation of the sensors, drift of the sensors output can occur over time. Additionally, the sensors can become damaged so that rows or columns of the 'sensels' no longer export forces. Saturation pressure (described above) is closely related to the calibration factor. Therefore, if some sensors become damaged during walking, the saturation pressure will change, and so this was tracked throughout the trials. A step calibration, which uses the test subject's weight to adjust the calibration factor was used to convert raw sum values into force measurement unit for each set of 5 consecutive trials. Fig. 14 shows a sample of saturation pressure record for the exemplar test subject. It can be seen that the accuracy of trials is reliable because the saturation pressures over 40 trials (a period of about 3 h) remain consistent.

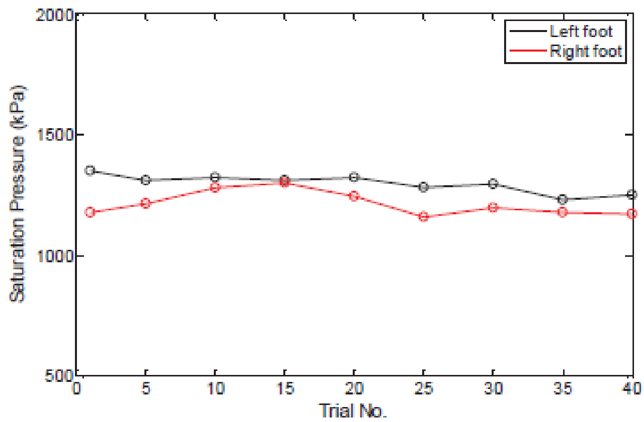

Figure 14: Little sensor degradation evidenced by almost constant saturation pressure across all trials for the exemplar test subject.

Due to the mentioned error involved in the Tekscan, and also the high accuracy of the force plate and load cells, the force plate and load cells are taken as the benchmark to check the reliability of the Tekscan results.

4. Main experimental results

4.1. Measured vibration response

Fig. 15a shows auto-spectral densities (ASDs) of the two accelerometers for the exemplar trial at resonance. Both ASDs can be seen to have high amplitudes at the first bending mode frequency of the footbridge (5.6 Hz) and at least two order of magnitudes lower amplitudes at other frequencies. The ASDs show that most of the footbridge vibration energy is distributed in the 5–6 Hz frequency range and originates from the first bending mode. They also indicate that there is little contribution from the first torsional mode since the magnitude of the ASDs are very close to zero at its frequency (around 9–10 Hz – see Fig. 15a). Thus, the mean of the two acceleration measurements is taken as the bridge vibration response at the mid-span. The frequency components of the response outside range of 5–6 Hz are removed for all trials using a zero-phase 4th order band-pass Butterworth filter (Fig. 15b). Zero-phase filtering avoids any time shift in the filtered signal.

High-frequency components are observed in the original measured acceleration signal, and it could be hypothesized that these come from the heel strike impulses of the pedestrian. However, the occurrence of heel strikes (as identified using TekScan) for the exemplar text subject are indicated as blue dashed lines in Fig. 15b, and do not coincide with the significant spikes in the signal. Thus, these high-frequency components are more likely related to other noise sources on the footbridge, such as the movements of the MDF boards. Humans are more sensitive to low-frequency vibrations [43], and consequently the footbridge vibration response outside of its first bending mode frequency range is filtered out in this work.

This paper has been published under the following reference: Ahmadi, E., Caprani, C., Živanović, S. and Heidarpour, A. (2018) Vertical ground reaction forces on rigid and vibrating surfaces for vibration serviceability assessment of structures. *Engineering Structures*, Vol. 172, pp. 723-738. (https://doi.org/10.1016/j.engstruct.2018.06.059)

The considered footbridge response metric is the maximum value of the footbridge vibration response, a_{max}. Maximum 1-s root-mean-square (RMS) could be used instead, but is directly proportional to the peak acceleration over a few cycles of vibration, and so response ratios are unaffected by the measure used. Fig. 16 shows the maximum acceleration response for all test subjects and trials, against the actual pacing frequency achieved. In Fig. 16a, the red dashed lines specify the previously defined boundaries for the resonant frequency range. The figure shows that the test subjects followed the metronome beat well since almost all actual pacing frequencies fall within their relevant range. The footbridge experiences maximum accelerations up to 3.3 m/s^2.

Acceleration levels are shown in Fig. 16b along with the limits in the Setra guideline [44], reproduced in Table 2. Table 2 clearly shows that in certain cases the footbridge provides "unacceptable discomfort" (CL4) to the occupants (7% of the walking trials) and, in many cases a "minimum comfort" (CL3, 32% of the walking trials).

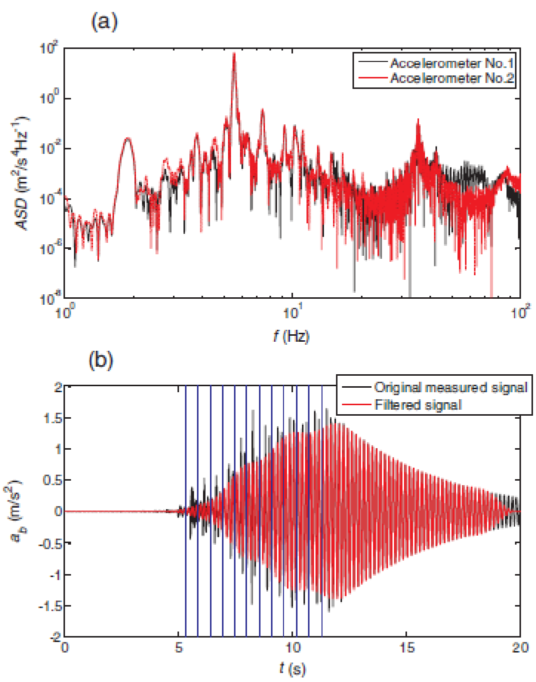

Figure 15: For the exemplar test subject no 1, trial no 9: (a) frequency content of the vibration response, and (b) mean acceleration response at the mid-span (the blue dashed lines show the feet location and the tapering at the end of the filtered signal is an artefact of the filter). (For interpretation of the references to colour in this figure legend, the reader is referred to the web version of this article.)

This paper has been published under the following reference: Ahmadi, E., Caprani, C., Živanović, S. and Heidarpour, A. (2018) Vertical ground reaction forces on rigid and vibrating surfaces for vibration serviceability assessment of structures. *Engineering Structures*, Vol. 172, pp. 723-738. (https://doi.org/10.1016/j.engstruct.2018.06.059)

It should be noted that even though the Setra acceleration limits were developed for vibrations up to 5 Hz, they are used here to characterize vibration levels since the vibration frequency of 5.6 Hz is not too far from the 5 Hz limit. In addition, the test subject's opinion about the vibration levels perceived was requested following each walking trial. The test subjects reported that the footbridge vibration was acceptable and occasionally affected the walking style in 25% of the trials, and the vibration was strong or uncomfortable and affected the walking style most of the time in 18% of the trials. This shows that the Monash University GFRP footbridge is considered to be a lively structure by some people and, as such, it is well-suited for studying human-induced vibration problems. In addition, it seems that the 5 Hz AASHTO limit might not provide adequate guidance for lightweight higher-frequency structures (Fig. 2).

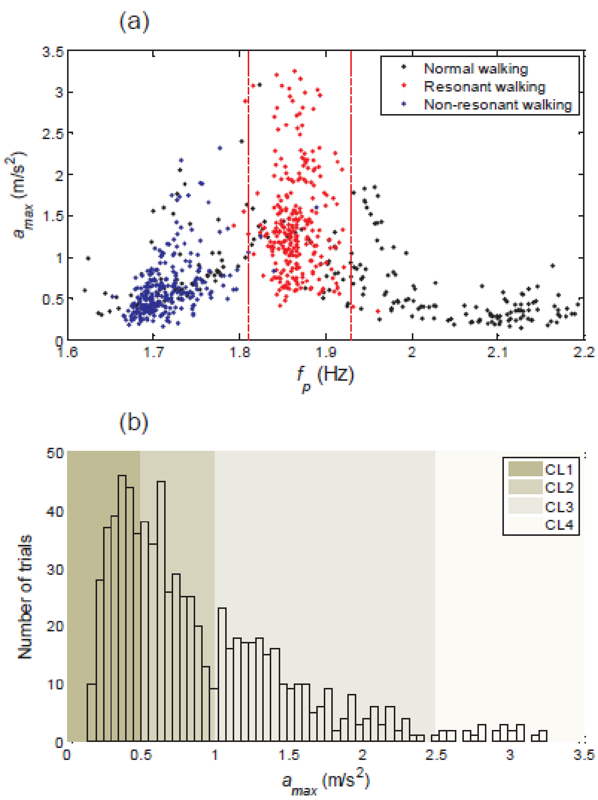

Figure 16: Footbridge vibration response for different: (a) true pacing frequencies (determined as described in Section 5.1), and (b) perception levels according to Setra [44] (Note that the resonant and non-resonant walking trials might not reflect natural walking situations as a metronome was used to adjust walking frequency).

This paper has been published under the following reference: Ahmadi, E., Caprani, C., Živanović, S. and Heidarpour, A. (2018) Vertical ground reaction forces on rigid and vibrating surfaces for vibration serviceability assessment of structures. *Engineering Structures*, Vol. 172, pp. 723-738. (https://doi.org/10.1016/j.engstruct.2018.06.059)

Table 2: Comfort levels and acceleration ranges [44].

Comfort level	Degree of comfort	Vertical acceleration limits (m/s^2)	Distribution of trial responses (%)
CL1	Maximum	< 0.5	29
CL2	Medium	0.5–1.0	32
CL3	Minimum	1.0–2.5	32
CL4	Unacceptable discomfort	> 2.5	7

4.2. Measured GRFs

Fig. 17 shows measured GRFs for the exemplar trial, from all three sets of measuring instruments. The force plate only measures one footstep due to its finite dimension on the bridge surface, while the load cells and Tekscan measure the total GRF continuously. Comparison of the three for the single step shows a good and consistent match, giving confidence in the measurements.

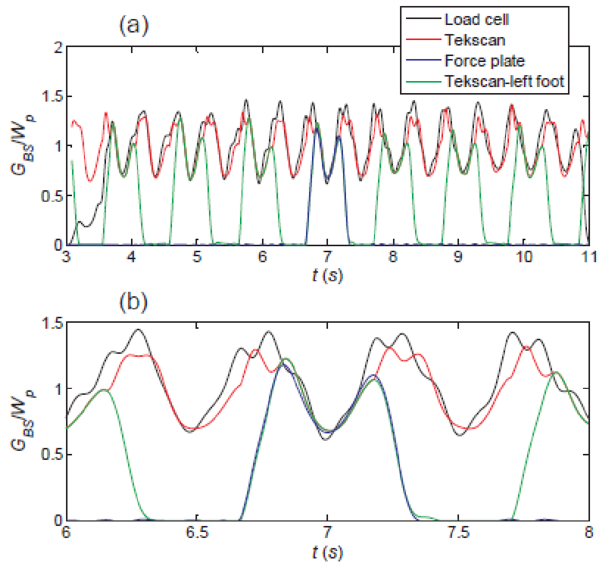

Figure 17: Exemplar force measurements by the load cells, force plate, and Tekscan: (a) full bridge walk, and (b) zoomed around the force plate reading.

Despite placing the force plate where it is highly likely to be hit by the test subjects, in some cases, the whole foot might not be on the force plate. To ensure that the force plate reading is from a full-contact footstep, three criteria were simultaneously considered numerically:

This paper has been published under the following reference: Ahmadi, E., Caprani, C., Živanović, S. and Heidarpour, A. (2018) Vertical ground reaction forces on rigid and vibrating surfaces for vibration serviceability assessment of structures. *Engineering Structures*, Vol. 172, pp. 723-738. (https://doi.org/10.1016/j.engstruct.2018.06.059)

1. Overall shape of vertical GRFs: the GRF shape should have two distinctive peaks (heel-strike and toe-off phases, $G_{\max1}$ and $G_{\max2}$) and a trough (mid-stance phase, $G_{\min}$), expressed as:

$$\frac{G_{max1}}{W_p} > 1;\quad \frac{G_{max2}}{W_p} > 1;\quad \frac{G_{min}}{W_p} < 1 \tag{8}$$

2. Step duration: the step duration from the force plate GRFs, t_{fp}, and the corresponding step from the Tekscan GRFs on the bridge surface, t_{ts}, should be similar:

$$\frac{|t_{fp}-t_{ts}|}{t_{ts}} \leqslant 0.1 \tag{9}$$

3. GRFs trajectory: the centre of pressure must remain within the force plate area.

A footstep is not a full-contact GRF if it fails any of these criteria. The location of the centre of pressure of the foot is calculated from the measured force and moment components of the force plate as:

$$x_{cp} = \frac{-hG_x - M_y}{G_z};\quad y_{cp} = \frac{-hG_y + M_x}{G_z} \tag{10}$$

where x_{cp} and y_{cp} are the coordinates of the centre of pressure relative to the coordinate axes of the force plate (Fig. 18) and h is the thickness above the top surface of any material covering the force plate (4 mm comprising 3mm MDF plus 1mm shim between the force plate and MDF sheeting). The origin of the coordinate system is centred on the top surface of the force plate (Fig. 18).

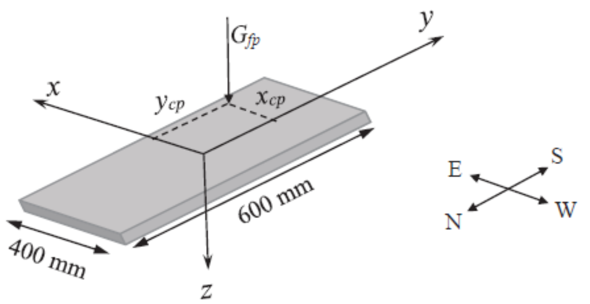

Figure 18: Force plate coordinate system along with the footbridge surface.

This paper has been published under the following reference: Ahmadi, E., Caprani, C., Živanović, S. and Heidarpour, A. (2018) Vertical ground reaction forces on rigid and vibrating surfaces for vibration serviceability assessment of structures. *Engineering Structures*, Vol. 172, pp. 723-738. (https://doi.org/10.1016/j.engstruct.2018.06.059)

Fig. 19a shows full-step force plate GRFs and one identified incomplete GRF as a negative example for the exemplar test subject at resonance. Considering criterion (1) above, the complete GRFs display two distinctive peaks for heel-strike and toe-off phases and a trough, mid-stance phase while the incomplete step clearly does not exhibit two peaks ($G_{max2}/W_p < 1$). For criterion (2), the contact time of the incomplete step is shorter than the duration of the same step as recorded in the GRF measured by Tekscan. Finally, for criterion (3), the GRF trajectories using Eq. (10) are shown in Fig. 19b for a few complete steps. The blue dashed line shows the force plate boundary. As seen, all GRF trajectories are within the force plate area. Each force trajectory starts from the force plate centre and ends at the same point, and the red dashed lines connect heel-strike to toe-off. However, for the incomplete GRF (shown in green), despite its force trajectory being within the force plate area, the overall shape of the GRF illustrates only the heel-strike phase, and the toe-off phase is outside the force plate (the red dashed line is very short). Although the number of incomplete GRF steps varies between different test subjects and walking frequencies, around 52% of all trials resulted in measurement of full GRF steps.

5. Detailed analysis of GRFs

In this section, all measured single-step GRFs and continuous walking GRFs are statistically analysed to examine effects of footbridge vibration on the walking force. Whenever appropriate, statistical hypothesis testing is performed to quantify the statistical significance of differences between variables. Two-sided independent sample Student's t-test and F-test are carried out to test the statistical significance of any difference between the mean and standard deviation of two sets of variables. The p-values from these tests are reported: small p-values show that differences in the mean or standard deviations of the two sets of variables are statistically significant, while high *p*-values indicate little statistically-meaningful difference.

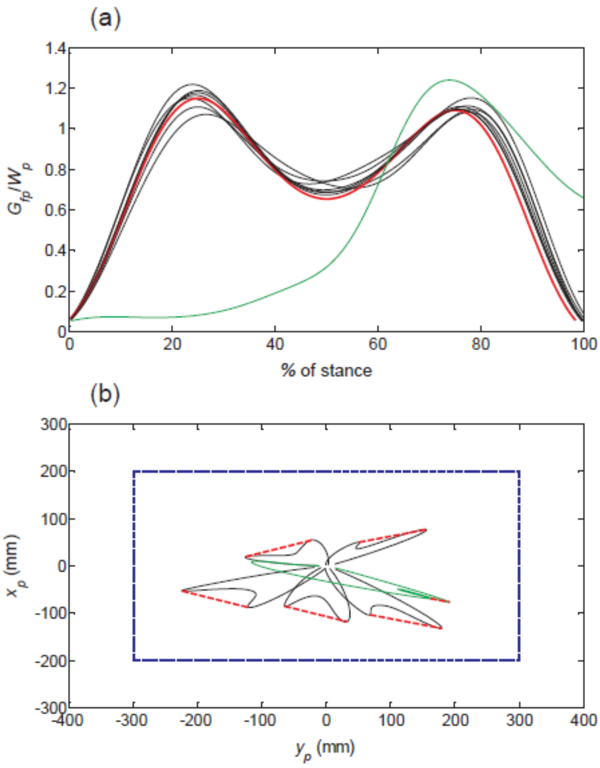

Figure 19: Identification of complete and incomplete steps on the force plate (the red one corresponds to the exemplar trial no. 9): (a) sample GRFs, and (b) centre of pressure trajectory on the force plate, and its criterion (red dashed lines connects heel-trike to toe-off and green one shows an incomplete step).

5.1. Pacing frequency analysis

Peaks from the Tekscan total GRF are used to determine the true pacing frequencies during each walking trial for the rigid and bridge surfaces (the load cells give almost identical results to the Tekscan for the bridge surface)—Fig. 20a shows the normalised GRF for the exemplar trial. The actual pacing periods for both surfaces, T_{BS} and T_{RS}, are determined using two consecutive peaks, and from them the pacing frequencies, as shown in Fig. 20b. The variability in the pacing frequencies even for just one walk for both BS and RS reflects intra-subject variability. For all tests subjects and trials, an average is taken across the measured pacing frequencies for the trial—the dashed lines in Fig. 20b—and is considered as the actual pacing frequency for the trial.

This paper has been published under the following reference: Ahmadi, E., Caprani, C., Živanović, S. and Heidarpour, A. (2018) Vertical ground reaction forces on rigid and vibrating surfaces for vibration serviceability assessment of structures. *Engineering Structures*, Vol. 172, pp. 723-738. (https://doi.org/10.1016/j.engstruct.2018.06.059)

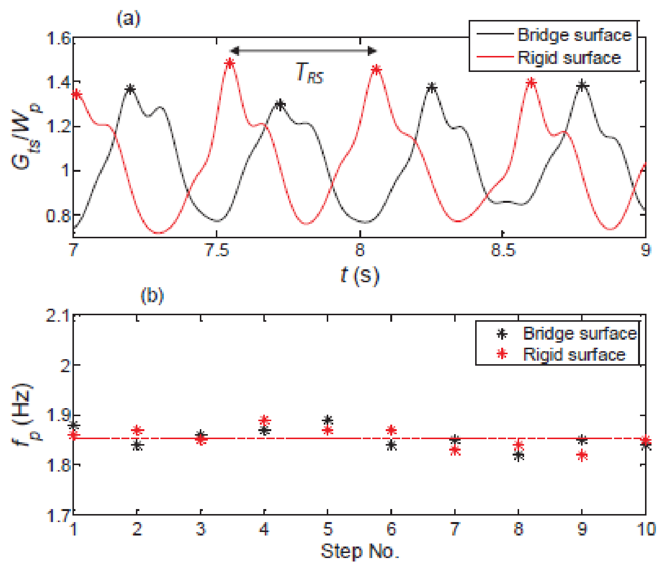

Figure 20: For the exemplar test subject and trial: (a) actual pacing periods, and (b) actual pacing frequencies.

Fig. 21a and 21b show actual pacing frequencies and target pacing frequencies for the rigid and bridge surfaces for all test subjects. The inter-subject variability in the data results in different level of success in matching the target frequency by different test subjects. The variability in mean actual pacing frequencies is low: the coefficient of variation, CoV (ratio of standard deviation to mean) is<0.009 for almost all test subjects. The exceptions are comparatively larger variations for test subject 1 on the rigid surface for non-resonant walk (CoV=0.038) and test subject 16 on the bridge surface for resonant walk (CoV=0.046). Small differences between the actual and target pacing frequencies is also observed typically. This means that test subjects, on average, synchronized their pacing frequencies quite well with the metronome beat (especially test subject 2). For uncontrolled normal walking pacing frequencies, the normal walking of test subjects 2, 7, 12, and 17 is close to resonance with the footbridge; for the remaining test subjects, it is out of resonance with the footbridge (see Fig. 21c).

Fig. 21d shows histograms of actual-to-target pacing frequency ratios for the rigid and bridge surfaces. The statistical parameters of the two distributions are summarized in Table 3. As

This paper has been published under the following reference: Ahmadi, E., Caprani, C., Živanović, S. and Heidarpour, A. (2018) Vertical ground reaction forces on rigid and vibrating surfaces for vibration serviceability assessment of structures. *Engineering Structures*, Vol. 172, pp. 723-738. (https://doi.org/10.1016/j.engstruct.2018.06.059)

seen, their mean and median are almost identical while results of the bridge surface have higher coefficients of variation.

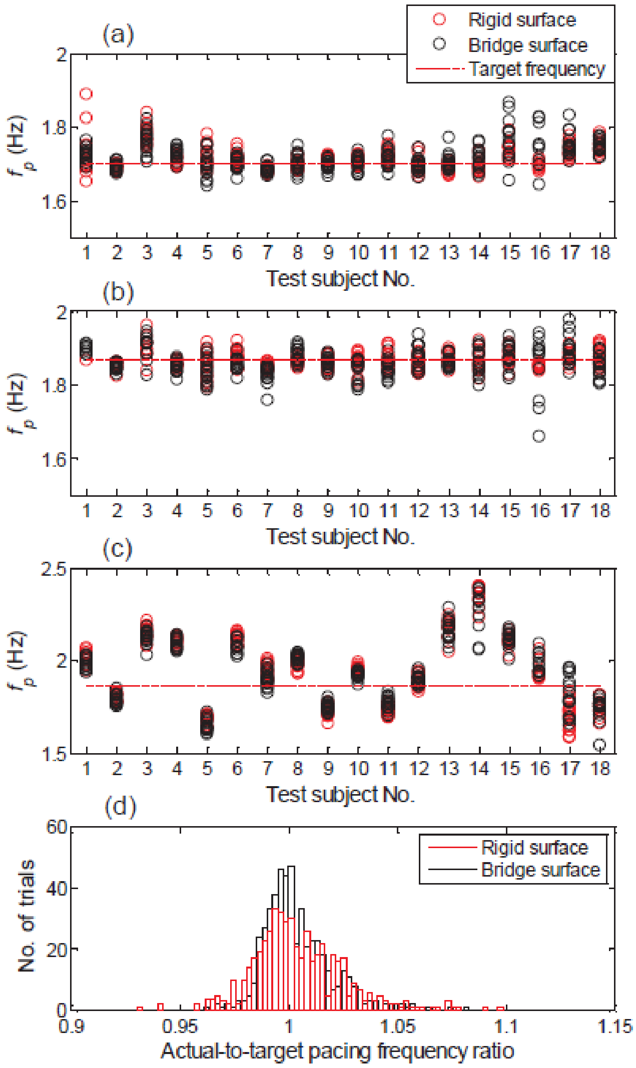

Figure 21: Actual pacing frequencies for: (a) non-resonant, (b) resonant, (c) normal walking pacing frequencies (red dashed line shows target pacing frequency, for normal walking it shows resonance target pacing frequency), and (d) actual-to-target pacing frequency ratio.

Table 3: Statistical parameters of actual-to-target pacing frequency ratios.

Surface type	Mean	Median	CoV
Rigid	1.004	1.000	0.016
Bridge	1.005	1.002	0.026

The *p*-values from the rigid and bridge surface pacing frequencies are 0.98 and 0.00 respectively for Student's t-test and F-test. These values show that the actual-to-target pacing frequency ratios on the bridge and rigid surfaces have no difference in their means but have a statistically significant difference in their standard deviations. This difference in standard deviation presumably indicates that the vibrating bridge surface makes it harder for the test subjects to maintain a set pacing frequency (according to the metronome beat). The results are similar to those found on a low-frequency footbridge [27] where the vibration effects on the mean of pacing frequencies was small while the effects on the CoV of pacing frequencies was higher.

5.2. Single-step GRFs

Single-step GRFs are not widely available in literature; however they are becoming of interest in discreet footfall moving force models in which the footstep forces are applied at the feet locations [45,46]. To inform development of single-step force models, complete single footsteps identified in Section 4.2 for all test subject trials are statistically analysed. To examine the footbridge vibration effects on the single-step GRFs, it is necessary to compare the footsteps on the rigid and bridge surfaces. The Tekscan GRFs on the bridge surface corresponding to the force plate GRFs are used (see Fig. 17). For Tekscan GRFs on the rigid surface, since they are not measured simultaneously with the GRFs on the bridge surface, it is not possible to find a corresponding step, and thus a representative step is randomly selected from the middle third of full-trial GRFs. Hence for each trial a comparison is made between randomly-selected single steps from the bridge and rigid surface measurements.

For time-domain analysis of single-step GRFs, the peak at heel strike, the peak at toe-off, and the trough at mid-stance were considered [2]. Vibration effects of the footbridge could not be clearly observed in the time-domain. Therefore, the single-step GRFs are compared in the frequency domain to understand the effect of vibration on individual footstep forces.

For frequency-domain analysis of step GRFs, a Fourier representation of single steps is used, [47]:

This paper has been published under the following reference: Ahmadi, E., Caprani, C., Živanović, S. and Heidarpour, A. (2018) Vertical ground reaction forces on rigid and vibrating surfaces for vibration serviceability assessment of structures. *Engineering Structures*, Vol. 172, pp. 723-738. (https://doi.org/10.1016/j.engstruct.2018.06.059)

$$G_s(t) = W_p \sum_{n=0}^{N} A_n \cos(2\pi n f_s t + \theta_n) \tag{11}$$

where A_n and θ_n are the nth harmonic and phase angle of the footstep; N is total number of harmonics considered; $f_s=1/t_s$ and t_s is the single step duration. The footstep frequency is proportional to the pacing frequency on average for all trials and test subjects, $f_s/f_p=0.82$, with the 95% confidence interval 0.82 ± 0.06. To calculate harmonics of single-step vertical GRFs, each one is repeated 10 times to form a longer periodic signal. This periodic signal is windowed using a Hann window to suppress leakage and zero-padded to increase its frequency resolution. It is then transformed to the frequency domain using the Fast Fourier Transform (FFT), and its amplitude in the frequency domain is corrected for the side-lobe loss due to using a spectral window [48]. Fig. 22 shows the DC component (A_0) and the first three harmonics of the force plate single-step GRF for the exemplar test subject and trial.

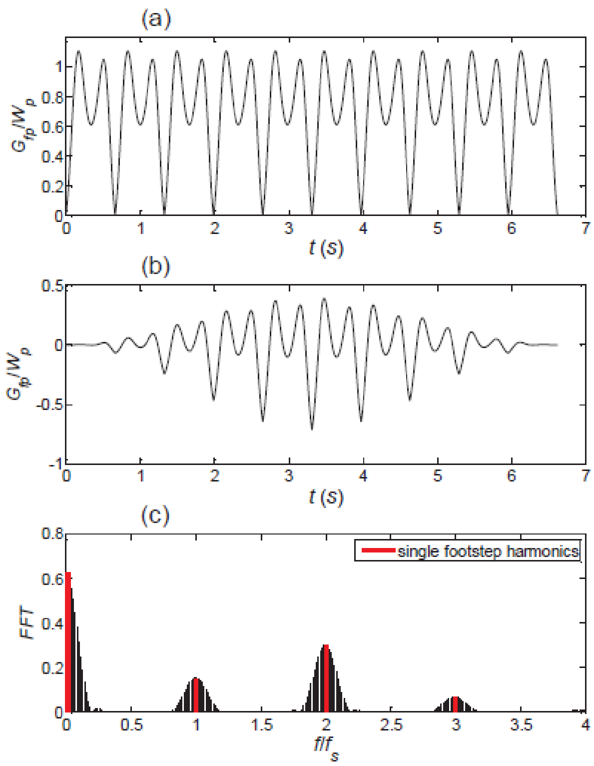

Figure 22: Single-step GRF harmonics: (a) repeated single-step GRF signal for the exemplary test subject, (b) windowed and trimmed repeated single-step GRF, and (c) Fast Fourier Transform of the trimmed repeated single-step GRF.

This paper has been published under the following reference: Ahmadi, E., Caprani, C., Živanović, S. and Heidarpour, A. (2018) Vertical ground reaction forces on rigid and vibrating surfaces for vibration serviceability assessment of structures. *Engineering Structures*, Vol. 172, pp. 723-738. (https://doi.org/10.1016/j.engstruct.2018.06.059)

The DC (constant) component and first three harmonics of all measured single-step GRFs on both surfaces are shown in Fig. 23. The red dashed lines show the resonant range of the footbridge. Visually, it appears the footbridge vibration reduces the third harmonic of single footsteps (Fig. 23d) and that the footbridge vibration effect on other harmonics seems negligible (Fig. 23a–c). This seems reasonable as the footstep frequency is proportional to pacing frequency, and for the resonant walking trials, the third harmonic of the single footsteps is closer to the bridge frequency compared to the other harmonics.

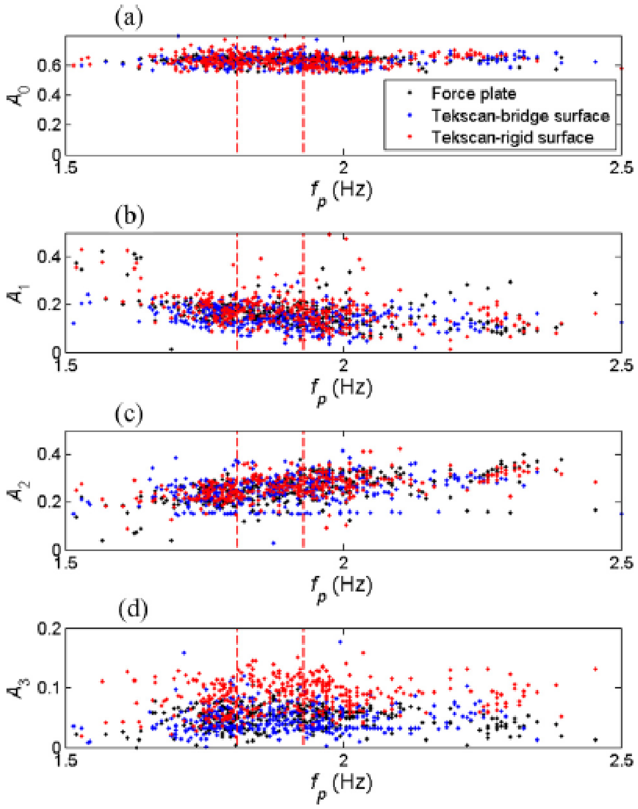

Figure 23: Relationships of single footstep harmonics with pacing frequency for: (a) DC component, (b) first harmonic, (c) second harmonic, and (d) third harmonic for all test subjects and trials.

The *p*-values for the footsteps harmonics are calculated for all test subjects and trials and are given in Table 4. Differences between the results of the load cells and Tekscan on the bridge surface shows any inaccuracy of Tekscan, while differences between the results of Tekscan on rigid and bridge surfaces is a relative indication of vibration effects on footstep harmonics. Note that it is assumed that any error in Tekscan measurements affects the results on both rigid and bridge surfaces in the same manner (especially in a statistical sense). This implies that the differences between the measurements on the two surfaces are solely due to influence of the surface itself. For bridge surface steps only, Table 4 shows that the Tekscan and force plate measured GRFs are consistent and do not exhibit statistically significant differences. In contrast, for the Tekscan results across the rigid and bridge surfaces, the results show an statistically-significant difference for the third harmonics of single footsteps. In this case the p-values observed are near zero ($\approx 10^{-7}$).

For representing vertical walking force in a single step it is useful to report the average magnitudes of each harmonic found, 0th–3rd, across all tests. As a proportion of body mass, for rigid surface walking these are 0.64, 0.18, 0.26, and 0.087 respectively, while for the bridge surface walk they are 0.63, 0.16, 0.25, and 0.047. Consequently, the mean reduction in third harmonic magnitude is about 46%.

Table 4: Hypothesis testing results (p-values) for single footstep harmonics for all trials and test subjects. (Recall the t-test examines differences in means, while the F-test examines differences in standard deviations. Values near zero indicate very high statistically-significant differences).

Harmonic no.	Bridge Surface only: Force plate and Tekscan		Tekscan only: Rigid and Bridge Surfaces	
	t-test	*F*-test	*t*-test	*F*-test
0	0.49	0.22	0.21	0.11
1	0.21	0.15	0.15	0.19
2	0.47	0.26	0.21	0.53
3	0.59	0.19	0.00	0.00

5.3. Continuous GRFs

To investigate vibration effects on continuous vertical GRFs, DLFs are selected as the metric, consistent with the literature [24–26,49]. DLFs of the first three harmonics are determined for

This paper has been published under the following reference: Ahmadi, E., Caprani, C., Živanović, S. and Heidarpour, A. (2018) Vertical ground reaction forces on rigid and vibrating surfaces for vibration serviceability assessment of structures. *Engineering Structures*, Vol. 172, pp. 723-738. (https://doi.org/10.1016/j.engstruct.2018.06.059)

full time history force of the load cells and Tekscan on both rigid and bridge surfaces. Comparison of the Tekscan and load cell differences for bridge surface walks are made to assess Tekscan accuracy as before. Comparison of the Tekscan measurements between the rigid and bridge surfaces are also made as before, to assess any influence of bridge vibration.

To calculate the DLFs from the GRF measurements, the start and end of the recorded GRF signals are trimmed such that a signal consists of an even number of full steps. The DC component is subtracted from the signal and it is then windowed using a Hann window to suppress leakage. Similar to the single footstep analysis, the signal is then zero-padded to increase its frequency resolution and transformed into the frequency domain using the FFT. The signal amplitude in the frequency domain is corrected for the side-lobe loss due to using a spectral window [48] as was done for the single footsteps. Fig. 24 shows the steps in determining DLFs for the exemplar trial, highlighting the first three harmonics. Consistent with past experiments, and as seen earlier in the intra-subject variability results, the walking force is not perfectly periodic but it is a narrow band signal with some of its energy spread to adjacent frequencies [17,18]. Subharmonics are also evident from Fig. 24c.

For each trial and surface (rigid and bridge surfaces), the first three DLFs of the continuous walking GRFs are calculated and shown in Fig. 25. For comparison, Kerr’s [50] upper and lower bounds for each DLF are shown by green dashed lines, and the vertical red dashed lines show the resonant range of the footbridge (Figs. 9 and 14a). The first DLF increases with increasing pacing frequency, while the second and third DLFs do not show a discernible trend as would be expected [50,51,15]. For the third harmonic of walking vertical force, the bridge DLFs on the bridge are lower than those on the rigid surface. Further, there is a difference between DLFs from the load cells and Tekscan measured on the bridge surface, emphasizing some error in the Tekscan force measurement.

This paper has been published under the following reference: Ahmadi, E., Caprani, C., Živanović, S. and Heidarpour, A. (2018) Vertical ground reaction forces on rigid and vibrating surfaces for vibration serviceability assessment of structures. *Engineering Structures*, Vol. 172, pp. 723-738. (https://doi.org/10.1016/j.engstruct.2018.06.059)

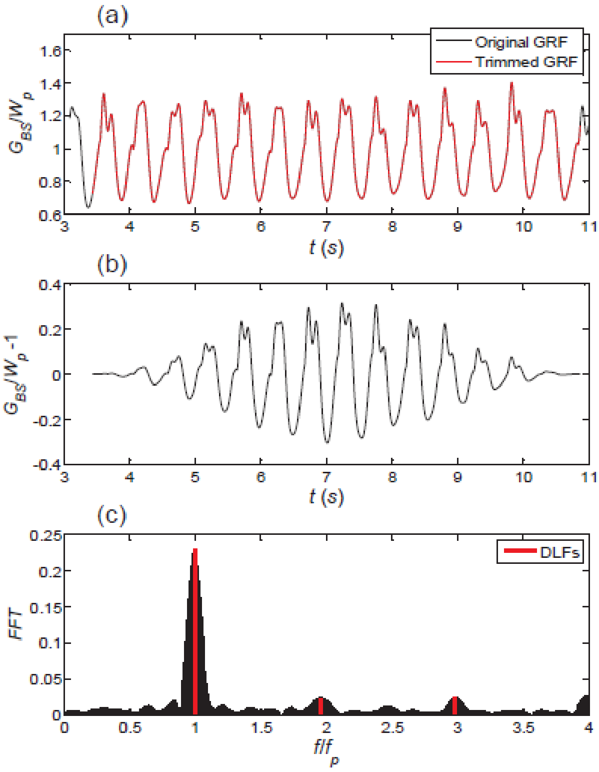

Figure 24: GRF DLFs: (a) bridge-measured Tekscan original and trimmed GRFs for the exemplary test subject and trial, (b) windowed trimmed GRF, and (c) Fast Fourier Transform of the trimmed and windowed GRF signal in (b).

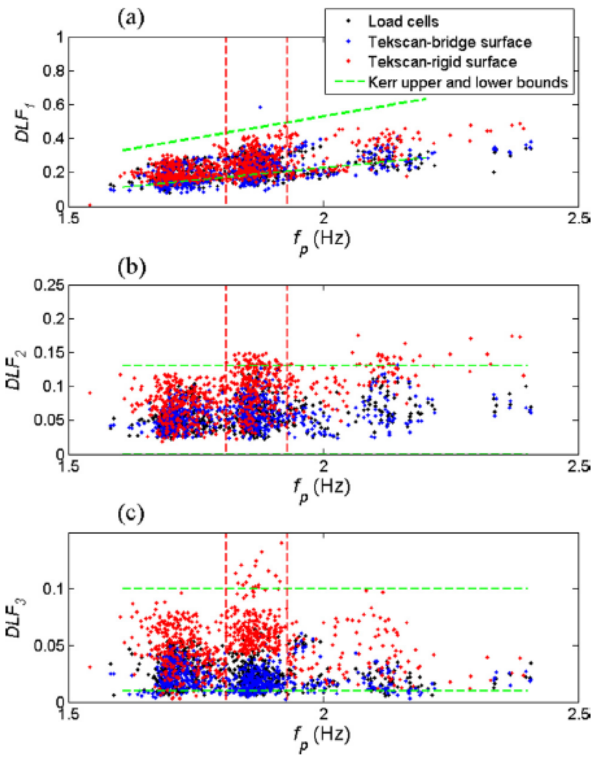

Figure 25: Relationships of DLFs with pacing frequency for: (a) first harmonic, (b) second harmonic, and (c) third harmonic for all test subjects and trials.

This paper has been published under the following reference: Ahmadi, E., Caprani, C., Živanović, S. and Heidarpour, A. (2018) Vertical ground reaction forces on rigid and vibrating surfaces for vibration serviceability assessment of structures. *Engineering Structures*, Vol. 172, pp. 723-738. (https://doi.org/10.1016/j.engstruct.2018.06.059)

The *p*-values for DLFs are calculated for all test subjects and trials and are given in Table 5. The *p*-values for the differences between the loads cells and Tekscan are not statistically significant but give an indication of the measurement error involved in using Tekscan. More interestingly, in the relative comparison of Tekscan results between the rigid and bridge surfaces: there are small *p*-values for the third DLF, indicating a statistically significant difference in both means and standard deviations. This suggests that the footbridge vibration affects the third harmonic far more than the first and second harmonics.

Table 5: Hypothesis testing results (p-values) for DLFs for all trials and test subjects. (Recall the t-test examines differences in means, while the F-test examines differences in standard deviations).

DLF no.	Bridge Surface only: Load cells and Tekscan		Tekscan only: Rigid and Bridge Surfaces	
	t-test	*F*-test	*t*-test	*F*-test
1	0.80	0.81	0.28	0.31
2	0.49	0.91	0.19	0.16
3	0.36	0.21	0.00	0.00

To compare the effects of the vibrating footbridge for the resonant and non-resonant pacing frequencies, the p-values between the bridge and rigid surface Tekscan DLFs are obtained for all test subjects, given in Table 6. As seen from this table, for both resonant and non-resonant walking, *p*-values of DLF1 and DLF2 are relatively high, illustrating little statistical difference between the DLFs of rigid and bridge surfaces for both resonant and non-resonant walking. However, for DLF3, again, very small *p*-values result, indicating significant differences in both mean and standard deviation for both resonant and non-resonant walking. This suggests that the footbridge vibration influences the nearest harmonic of walking force for any pacing frequency. This phenomenon is explored next.

To analyse the DLFs in more detail, p-values of the first three DLFs are obtained for each test subject at the resonant and non-resonant pacing frequencies (see Tables 7–9). These are based

This paper has been published under the following reference: Ahmadi, E., Caprani, C., Živanović, S. and Heidarpour, A. (2018) Vertical ground reaction forces on rigid and vibrating surfaces for vibration serviceability assessment of structures. *Engineering Structures*, Vol. 172, pp. 723-738. (https://doi.org/10.1016/j.engstruct.2018.06.059)

on the statistics of the GRFs from 15 trials at each pacing frequency for each test subject. The test subject-to-footbridge mass ratio, μ, is used to discuss the results for each test subject. Again, very small p-values are observed for the third harmonic compared to the other two harmonics for all test subjects. This is strong evidence that the effects of the footbridge vibration on the third harmonic is significant. Further, the effect roughly increases with increasing mass ratio. On the other hand, the first and second harmonics are not influenced much by vibration since their *p* values are high, on average.

Table 6: Hypothesis testing results (p-values) for DLFs for all trials and test subjects in resonant and non-resonant cases. (Recall the t-test examines differences in means, while the F-test examines differences in standard deviations).

DLF no.	Resonant		Non-resonant	
	t-test	*F*-test	*t*-test	*F*-test
1	0.28	0.14	0.55	0.05
2	0.19	0.98	0.11	0.64
3	0.00	0.00	0.00	0.01

Table 7: The first DLFs hypothesis testing results (p-values) and increment for each test subject in resonant and non-resonant cases. (Recall the t-test examines differences in means, while the F-test examines differences in standard deviations).

μ (%)	Resonant			Non-resonant		
	t-test	*F*-test	Δ_{DLF} (%)	*t*-test	*F*-test	Δ_{DLF} (%)
4.8	0.04	0.00	4.6	0.45	0.43	−0.3
5.4	0.18	0.31	4.5	0.95	0.15	−0.9
5.5	0.23	0.33	3.	0.64	0.05	3.7
5.7	0.15	0.02	5.2	0.55	0.07	2.1
6.6	0.23	0.33	4.9	0.95	0.12	3.5
7.0	0.04	0.01	3.6	0.45	0.04	4.0
7.3	0.00	0.04	6.0	0.30	0.76	2.4
7.4	0.15	0.39	3.0	0.73	0.08	1.9
7.4	0.13	0.20	5.2	0.42	0.24	2.1
7.8	0.27	0.11	5.1	0.85	0.11	2.6
7.8	0.14	0.02	6.3	0.56	0.10	2.3
8.4	0.14	0.33	4.2	0.68	0.21	1.2
9.3	0.04	0.85	3.6	0.97	0.35	0.2
9.4	0.03	0.07	3.0	0.32	0.25	−0.2
10.6	0.13	0.03	2.8	0.62	0.08	−1.2
11.6	0.12	0.02	3.3	0.43	0.05	−0.9
12.1	0.54	0.64	2.4	0.73	0.74	−1.5
16.2	0.29	0.13	2.3	0.55	0.04	−1.5

This paper has been published under the following reference: Ahmadi, E., Caprani, C., Živanović, S. and Heidarpour, A. (2018) Vertical ground reaction forces on rigid and vibrating surfaces for vibration serviceability assessment of structures. *Engineering Structures*, Vol. 172, pp. 723-738. (https://doi.org/10.1016/j.engstruct.2018.06.059)

Table 8: The second DLFs hypothesis testing results (p-values) and increment for each test subject in resonant and non-resonant cases. (Recall the t-test examines differences in means, while the F-test examines differences in standard deviations).

μ (%)	Resonant			Non-resonant		
	t-test	F-test	Δ_{DLF} (%)	t-test	F-test	Δ_{DLF} (%)
4.8	0.19	0.00	−6.7	0.09	0.57	−3.6
5.4	0.01	0.19	−2.3	0.02	0.87	−3.7
5.5	0.17	0.72	−5.4	0.12	0.37	−4.0
5.7	0.03	0.18	−4.6	0.02	0.77	−6.7
6.6	0.10	0.95	−3.8	0.03	0.71	−5.4
7.0	0.00	0.01	−5.5	0.01	0.90	−8.1
7.3	0.11	0.00	−4.2	0.07	0.73	−5.2
7.4	0.14	0.74	−3.2	0.09	0.41	−6.4
7.4	0.12	0.00	−6.5	0.03	0.60	−5.3
7.8	0.81	0.74	−5.0	0.66	1.00	−4.3
7.8	0.02	0.00	−4.6	0.07	0.86	−3.9
8.4	0.01	0.05	−2.3	0.01	0.88	−1.8
9.3	0.45	0.06	−5.9	0.85	0.88	−2.4
9.4	0.06	0.00	−6.8	0.09	0.70	−5.2
10.6	0.01	0.00	−6.0	0.00	0.41	−6.5
11.6	0.03	0.14	−6.0	0.04	0.77	−6.9
12.1	0.10	0.30	−6.3	0.92	0.25	−6.7
16.2	0.13	0.72	−5.4	0.10	0.51	−6.4

Table 9: The third DLFs hypothesis testing results (p-values) and increment for each test subject in resonant and non-resonant cases. (Recall the t-test examines differences in means, while the F-test examines differences in standard deviations).

μ (%)	Resonant			Non-resonant		
	t-test	F-test	Δ_{DLF} (%)	t-test	F-test	Δ_{DLF} (%)
4.8	0.01	0.00	−24.6	0.01	0.01	−12.9
5.4	0.00	0.00	−23.8	0.00	0.01	−11.1
5.5	0.00	0.00	−21.4	0.00	0.01	−11.2
5.7	0.00	0.00	−21.3	0.01	0.00	−13.0
6.6	0.00	0.00	−25.7	0.00	0.01	−17.0
7.0	0.00	0.00	−29.6	0.00	0.00	−16.4
7.3	0.01	0.00	−30.4	0.00	0.07	−16.5
7.4	0.00	0.00	−28.7	0.00	0.02	−15.4
7.4	0.00	0.00	−28.9	0.04	0.05	−14.9
7.8	0.00	0.00	−27.5	0.00	0.30	−15.5
7.8	0.00	0.00	−26.2	0.01	0.03	−15.6
8.4	0.00	0.00	−27.7	0.00	0.00	−17.2
9.3	0.00	0.00	−28.9	0.01	0.32	−18.8
9.4	0.00	0.00	−28.5	0.02	0.03	−18.4
10.6	0.00	0.00	−25.3	0.01	0.01	−17.6
11.6	0.00	0.00	−23.6	0.01	0.00	−16.8
12.1	0.00	0.00	−28.6	0.00	0.27	−18.4
16.2	0.00	0.00	−28.8	0.00	0.01	−19.2

Tables 7–9 also present relative changes in the mean DLFs, ΔDLF:

This paper has been published under the following reference: Ahmadi, E., Caprani, C., Živanović, S. and Heidarpour, A. (2018) Vertical ground reaction forces on rigid and vibrating surfaces for vibration serviceability assessment of structures. *Engineering Structures*, Vol. 172, pp. 723-738. (https://doi.org/10.1016/j.engstruct.2018.06.059)

$$\Delta_{DLF_i}(\%) = 100\frac{(\overline{DLF}_i^{BS} - \overline{DLF}_i^{RS})}{\overline{DLF}_i^{RS}} \quad (12)$$

where $\overline{DLF}_i^{BS}$ and $\overline{DLF}_i^{RS}$ RS are mean DLFs (across the 15 trials) for the ith harmonic. For DLF_3, a significant drop is seen for both resonant and non-resonant cases. Apart from this, DLF_3 reductions at the resonant walking are larger than those for the non-resonant walking, emphasizing high footbridge vibration effects at the resonant walking. As evident from Fig. 14a, the footbridge experiences high vibration response even at the non-resonant walking particularly for heavy test subjects. Considering that the footbridge vibration response is distributed over the range of 5–6 Hz (Section 4.1, Fig. 13a), the footbridge vibration is seen to clearly affect the third harmonics of the non-resonant walking force, but not as significantly as it affects the resonant walking force.

It is worth noting that similar reductions in DLFs close to the bridge frequency were found in trials on the low-frequency Warwick footbridge [27]. A possible explanation for these reductions is that similar to a stationary human [43,2], a moving human also applies an interaction force to the structure, i.e., G_V, proportional to the structural acceleration [52,2]. With this concept, there are two components combining to give the GRF on the bridge surface, G_{BS}: the rigid surface force, G_{RS}, and a vibrating surface force component, G_V :

$$G_{BS} = G_{RS} + G_V \quad (13)$$

For the higher-frequency Monash footbridge, the vibrating surface force component still exists at non-resonant pacing frequencies (according to the non-resonant pacing frequency results). In contrast, for the low-frequency Warwick footbridge, the vibrating surface walking force is similar to that of the rigid surface (very similar DLFs) and so the vibrating surface force component (GV component in Eq. (13)) is negligible. Since other factors are accounted for, this difference is most likely due to the different human-to-structure mass ratios. The Monash footbridge is far lighter than the Warwick footbridge and has much higher accelerance (see Fig. 2). Consequently, it seems that heavier test subjects can highly vibrate the footbridge even at non-resonant pacing frequencies (Fig. 14a).

6. Conclusions

In this paper, a novel experimental approach is introduced to quantify the extent of human-structure interaction on lightweight bridges with natural frequency above 5 Hz. A purpose-built higher frequency GFRP footbridge was used for walking trials. A unique experimental setup was designed to measure vertical walking forces on both rigid and flexible surfaces. This setup enables measuring both single-step and continuous GRFs on both a rigid surface and a vibrating bridge surface for 18 test subjects and trials. In addition, during walk over the bridge, vibration of the structure is also recorded.

It is consistently found that the vibrating bridge surface causes a statistically significant drop in the magnitude of the walking force harmonic closest to the vibration frequency. The amount of the reduction depends on whether the pacing frequency is such to cause a resonant or non-resonant condition between the relevant bridge frequency and walking harmonic. This result is similar to some results from a study on a low-frequency bridge. The findings support the hypothesis that the bridge surface vibration significantly decreases the magnitude of the harmonic of walking force that is closest to the vibration frequency. Further, it is also found that pacing frequencies vary more on a vibrating surface than on a rigid surface. Currently, these aspects are not considered in design guidelines and could be of significance in more accurately predicting vibration serviceability of lightweight structures.

Finally, the results of the trials conducted here show that the 5 Hz recommendation for FRP bridges provided by AASHTO performs poorly. The Monash GFRP footbridge reaches uncomfortable vibration levels even though the footbridge frequency is higher than 5 Hz. Therefore, it is necessary to develop more suitable design criteria for FRP bridges, or indeed, any lightweight bridge characterised by high magnitude of the accelerance function.

ACKNOWLEDGMENT

This work was funded by a Monash-Warwick Alliance Seed Grant and a Monash Graduate Scholarship (MGS). The third author also acknowledges support received by the UK Engineering and Physical Sciences Research Council [grant number EP/M021505/1: *Characterising Dynamic Performance of Fibre Reinforced Polymer Structures for Resilience and Sustainability*].

7. References

[1] Fujino Y, Pacheco BM, Nakamura S, Warnitchai P. Synchronization of human walking observed during lateral vibration of a congested pedestrian bridge. Earthq Eng Struct Dyn 1993;22:741–58. http://dx.doi.org/10.1002/eqe.4290220902.

[2] Racic V, Pavic A, Brownjohn JMW. Experimental identification and analytical modelling of human walking forces: literature review. J Sound Vib 2009;326:1–49. http://dx.doi.org/10.1016/j.jsv.2009.04.020.

[3] Younis A, Avci O, Hussein M, Davis B, Reynolds P. Dynamic forces induced by a single pedestrian: a literature review. Appl Mech Rev 2017;69. http://dx.doi.org/10.1115/1.4036327.

[4] Živanović S, Pavic A, Reynolds P. Vibration serviceability of footbridges under human-induced excitation: a literature review. J Sound Vib 2005;279:1–74. http://dx.doi.org/10.1016/j.jsv.2004.01.019.

[5] Kala J, Salajka V, Hradil P. Footbridge response on single pedestrian induced vibration analysis. World Acad Sci Eng Technol 2009;3:744–55.

[6] Galbraith FW. Ground loading from footsteps. J Acoust Soc Am 1970;48:1288. http://dx.doi.org/10.1121/1.1912271.

This paper has been published under the following reference: Ahmadi, E., Caprani, C., Živanović, S. and Heidarpour, A. (2018) Vertical ground reaction forces on rigid and vibrating surfaces for vibration serviceability assessment of structures. *Engineering Structures*, Vol. 172, pp. 723-738. (https://doi.org/10.1016/j.engstruct.2018.06.059)

[7] Andriacchi TP, Ogle JA, Galante JO. Walking speed as a basis for normal and abnormal gait measurements. J Biomech 1977;10:261–8.

[8] Bachmann H, Ammann W. Vibrations in structures—induced by man and machines, structural engineering documents, international association of bridge and structural engineering (IABSE). Zurich; 1987.

[9] Ebrahimpour A, Hamam A, Sack RL, Patten WN. Measuring and modeling dynamic loads imposed by moving crowds. J Struct Eng 1996;122:1468–74. http://dx.doi.org/10.1061/(ASCE)0733-9445(1996) 122:12(1468).

[10] Sahnaci C, Kasperski M. Prediction of the vibrations of pedestrian structures under random pedestrian streams. In: 9th int conf struct dyn EURODYN, Porto, Portugal; 2014. p. 1065–72.

[11] Tuan CY, Saul WE. Loads due to spectator movements. J Struct Eng 1985;111:418–34. http://dx.doi.org/10.1061/(ASCE)0733-9445(1985) 111:2(418).

[12] Ebrahimpour A, Sack RL. Modeling dynamic occupant loads. J Struct Eng 1989;115:1476–96. http://dx.doi.org/10.1061/(ASCE)0733-9445(1989) 115:6(1476).

[13] Ebrahimpour A, Sack RL, Van Kleek PD. Computing crowd loads using a nonlinear equation of motion. Comput Struct 1991;41:1313–9. http://dx.doi.org/10.1016/0045-7949(91)90268-Q.

[14] Živanović S, Pavić A, Reynolds P. Probability-based prediction of multi-mode vibration response to walking excitation. Eng Struct 2007;29:942–54. http://dx.doi.org/10.1016/j.engstruct.2006.07.004.

[15] Brownjohn JM, Pavic A, Omenzetter P. A spectral density approach for modelling continuous vertical forces on pedestrian structures due to walking. Can J Civ Eng 2004;31:65–77. http://dx.doi.org/10.1139/l03-072.

[16] Piccardo G, Tubino F. Simplified procedures for vibration serviceability analysis of footbridges subjected to realistic walking loads. Comput Struct 2009;87:890–903. http://dx.doi.org/10.1016/j.compstruc.2009.04.006.

[17] Caprani CC. A modal precise integration method for the calculation of footbridge vibration response. Comput Struct 2013;128:116–27. http://dx.doi.org/10.1016/j.compstruc.2013.06.006.

[18] Racic V, Brownjohn JMW. Mathematical modelling of random narrow band lateral excitation of footbridges due to pedestrians walking. Comput Struct 2012;90:116–30. http://dx.doi.org/10.1016/j.compstruc.2011.10.002.

[19] Racic V, Brownjohn JMW. Stochastic model of near-periodic vertical loads due to humans walking. Adv Eng Inform 2011;25:259–75. http://dx.doi.org/10.1016/j.aei.2010.07.004.

[20] Rainer JH, Pernica G, Allen DE. Dynamic loading and response of footbridges. Can J Civ Eng 1988;15:66–71. http://dx.doi.org/10.1139/l88-007.

[21] Yao S, Wright JR, Pavic A, Reynolds P. Forces generated when bouncing or jumping on a flexible structure. ISMA, vol. 2, Leuven, Belgium; 2002. p. 563–72.

[22] Wheeler JE. Prediction and control of pedestrian-induced vibration in footbridges. ASCE J Struct Div 1982;108:2045–65..

[23] Caprani CC, Ahmadi E. Formulation of human-structure system models for vertical vibration. J Sound Vib 2016. http://dx.doi.org/10.1016/j.jsv.2016.05.015.

[24] Ohlsson SV. Floor vibrations and human discomfort, PhD Thesis, Goteborg, Sweden. Chalmers University of Technology; 1982.

[25] Baumann K, Bachmann H. Durch menschen verursachte dynamische lasten und deren auswirkungen auf balkentragwerke. Zurich, Switzerland: Swiss Federal Institute of Technology (ETH); 1988.

[26] Pimentel RL. Vibrational performance of pedestrian bridges due to human-induced loads. Sheffield, UK: University of Sheffield; 1997.

[27] Dang HV, Živanović S. Influence of low-frequency vertical vibration on walking locomotion; 2015. p. 1–12. http://doi.org/10.1061/(ASCE)ST.1943-541X.0001599.

[28] Živanović S, Wei X, Russell J, Mottram JT. Vibration performance of two FRP footbridge structures in the United Kingdom. Footbridge 2017 Berlin – tell a story conf proc 6-892017 TU-Berlin; 2017. http://doi.org/10.24904/footbridge2017.09384.

[29] (AASHTO), American Association of State Highway and Transportation Officials. Guide specifications for design of FRP pedestrian bridges; 2008.

[30] The Highways Agency. Design of FRP bridges and highway structures; 2005.

[31] Živanović S, Feltrin G, Mottram JT, Brownjohn JMW. Vibration performance of bridges made of fibre reinforced polymer. IMAC-XXXII, Orlando, Florida, USA; 3–6 February 2014. p. 155–62. http://doi.org/10.1007/978-1-4419-9831-6.

[32] Bertec Corporation. user manual; 2012. http://bertec.com.

[33] HBM Corporation. user manual; 2017. https://www.hbm.com.

[34] Tekscan. Force measurement and tactile sensors; 2017. https://www.tekscan.com.

[35] Forner Cordero A, Koopman HJFM, Van Der Helm FCT. Use of pressure insoles to calculate the complete ground reaction forces. J Biomech 2004;37:1427–32. http://dx.doi.org/10.1016/j.jbiomech.2003.12.016.

[36] Fong DTP, Chan YY, Hong Y, Yung PSH, Fung KY, Chan KM. Estimating the complete ground reaction forces with pressure insoles in walking. J Biomech 2008;41:2597–601. http://dx.doi.org/10.1016/j.jbiomech.2008.05.007.

[37] Drewniak EI, Crisco JJ, Spenciner DB, Fleming BC. Accuracy of circular contact area measurements with thin-film pressure sensors. J Biomech 2007;40:2569–72. http://dx.doi.org/10.1016/j.jbiomech.2006.12.002.

This paper has been published under the following reference: Ahmadi, E., Caprani, C., Živanović, S. and Heidarpour, A. (2018) Vertical ground reaction forces on rigid and vibrating surfaces for vibration serviceability assessment of structures. *Engineering Structures*, Vol. 172, pp. 723-738. (https://doi.org/10.1016/j.engstruct.2018.06.059)

[38] Zammit GV, Menz HB, Munteanu SE. Reliability of the TekScan MatScan®system for the measurement of plantar forces and pressures during barefoot level walking in healthy adults. J Foot Ankle Res 2010;3:1–9. http://dx.doi.org/10.1186/1757-1146-3-11.

[39] Barnett S, Cunningham JL, West S. A comparison of verical force and temporal parameters produced by an in-shoe pressure measuring system and a force platform – Barnett.pdf 2001;16:353–7.

[40] Brimacombe JM, Wilson DR, Hodgson AJ, Ho KCT, Anglin C. Effect of calibration method on Tekscan sensor accuracy. J Biomech Eng 2009;131:34503. http://dx.doi.org/10.1115/1.3005165.

[41] Lu H, Lin G. An investigation of various factors affecting measurement accuracy of the Tekscan seat pressure system. Proc Hum Factors Ergon Soc Annu Meet 1996;40:1036–40. http://dx.doi.org/10.1177/154193129604002006.

[42] Data Translation. A measurment computing company; 2017. http://www.datatranslation.eu.

[43] Griffin MJ, Erdreich J. Handbook of human vibration. J Acoust Soc Am 1991;90:2213. http://dx.doi.org/10.1121/1.401606.

[44] Sétra, Guide methodologique passerelles pietonnes (technical guide footbridges: assessment of vibrational behaviour of footbridges under pedestrian loading); 2006.

[45] Yin Shih-Hsun. Vibration assessment of a simply supported footbridge under discrete pedestrian loading. Chinese Inst Eng 2017;40:503–13. http://dx.doi.org/10.1080/02533839.2017.1347062.

[46] Bard D, Sonnerup J, Sandberg GG, Persson K, Sandberg GG, Sonnerup J, et al. Human footsteps induced floor vibration. J Acoust Soc Am 2008;123:3356. http://dx.doi.org/10.1121/1.2933932.

[47] Li Q, Fan J, Nie J, Li Q, Chen Y. Crowd-induced random vibration of footbridge and vibration control using multiple tuned mass dampers. J Sound Vib 2010;329:4068–92. http://dx.doi.org/10.1016/j.jsv.2010.04.013.

[48] Bendat JS, Piersol AG. Random data: analysis and measurement procedures. Wiley series in probability and statistics; 2009.

[49] Toso MA, Gomes HM, da Silva FT, Pimentel RL. Experimentally fitted biodynamic models for pedestrian-structure interaction in walking situations. Mech Syst Signal Process 2015;72–73:590–606. http://dx.doi.org/10.1016/j.ymssp.2015.10.029.

[50] Kerr SC. Human induced loading on staircases; 1998. http://doi.org/10.1016/S0141-0296(00)00020-1.

This paper has been published under the following reference: Ahmadi, E., Caprani, C., Živanović, S. and Heidarpour, A. (2018) Vertical ground reaction forces on rigid and vibrating surfaces for vibration serviceability assessment of structures. *Engineering Structures*, Vol. 172, pp. 723-738. (https://doi.org/10.1016/j.engstruct.2018.06.059)

[51] Young P. Improved floor vibration prediction methodologies, ARUP vibration seminar; 2001.

[52] Bocian M, Macdonald JHG, Burn JF. Biomechanically inspired modeling of pedestrian-induced vertical self-excited forces. J Bridg Eng 2013;18:1336–46. http://dx.doi.org/10.1061/(ASCE)BE.1943-5592.0000490.